OFFICE OF CIVILIAN RADIOACTIVE WASTE MANAGEMENT

CALCULATION COVER SHEET

1. QA: QA
Page: 1 Of: 38

2. Calculation Title
Radiolytic Specie Generation from Internal Waste Package Criticality

MOL.20011017.0090

3. Document Identifier (including Revision Number)
CAL-EBS-NU-000017 REV 00

4. Total Attachments	5. Attachment Numbers – Number of pages in each
3	I-1, II (1 + CD-ROM), III-12

	Print Name	Signature	Date
6. Originator	John A. McClure Georgeta Radulescu	John A McClure Georgeta Radulescu	9/25/2001 9/28/2001
7. Checker	Luca J. Gratton (Technical) Kristine Dutton (Compliance)	Luca J. Gratton Kristine Dutton	9/28/2001 9/28/01
8. Lead	John A. McClure	John A McClure	9/25/2001

9. Remarks

Revision History

10. Revision No.	11. Description of Revision
00	Initial Issue

CONTENTS

FIGURES

Page

TABLES

ACRONYMS

B&W	Babcock and Wilcox
BSC	Bechtel SAIC Company
BWR	Boiling Water Reactor
CD-ROM	Compact Disc - Read Only Memory
CRWMS	Civilian Radioactive Waste Management System
CSNF	Commercial Spent Nuclear Fuel
DHLW	Department of Energy Owned High Level Waste
DOE	U.S. Department of Energy
DTN	Data Tracking Number
EBS	Engineered Barrier System
FEP	Features, Events, and Processes
GWd/MTU	GigaWatt days per Metric Ton Uranium
k_{eff}	effective neutron multiplication number
MGR	Monitored Geologic Repository
M&O	Management and Operating Contractor
NRC	U.S. Nuclear Regulatory Commission
OCRWM	Office of Civilian Radioactive Waste Management
PWR	Pressurized Water Reactor
SNF	Spent Nuclear Fuel
WP	Waste Package
YMP	Yucca Mountain Project

1. PURPOSE

The effects of radiation on the corrosion of various metals and alloys, particularly with respect to in-reactor processes, has been discussed by a number of authors (Shoesmith and King 1998, p. 2). Shoesmith and King (1998) additionally discuss the effects of radiation on the proposed Monitored Geologic Repository (MGR) Waste Package (WP) materials. Radiation effects on the corrosion of metals and alloys include, among other things, radiolysis of the local gaseous and aqueous environment to produce both oxidizing and reducing radicals. In particular, radiolysis processes in moist air environments lead to the fixation of nitrogen as NO, NO_2, and especially HNO_3 (Reed and Van Konynenburg 1988, pp. 393-404). Nitric acid is assumed to be the principal corrosive radiolytic chemical specie and is produced in an irradiated air-water vapor system when the hydroxyl radicals generated from the water vapor convert nitrogen dioxides, that are formed by the radiolytic reaction between nitrogen and oxygen, to nitric acids.

Chemical species produced by radiolysis have been identified in the Disposal Criticality Analysis Methodology Topical Report (DCTR) (YMP 2000, p. 2-2) as a mechanism for accelerating corrosion of the MGR engineered barrier system (EBS). Radiolytic sources of corrosion have also been considered in the screening of processes and issues in the drip shield and WP degradation (Civilian Radioactive Waste Management System [CRWMS] Management and Operating Contractor [M&O] 2001a, Section 6.2.27), Yucca Mountain Project (YMP) features, events, and processes (FEP) No. 2.1.13.01.00. The latter reference dealt specifically with radiolytic effects of gamma radiation on the WP and drip shield, excluding them from further consideration because of low consequence. The potential for chemical interactions within the WP from radiolytic effects was considered insignificant in the Waste Form Degradation Process Model Report (CRWMS M&O 2000c, p. 3-21) and therefore neglected except as a possible perforation mechanism for the Zircaloy cladding (CRWMS M&O 2000c, p. 3-40).

Radiolysis producing a local depression of the pH resulting in localized corrosion of cladding material is included in the localized corrosion model as a special feature, YMP FEP NO. 2.1.02.15.00 (CRWMS M&O 2000d, Section 6.2.5). Neutron and gamma doses considered in the screening decision for this FEP were representative of the residual radionuclide decay only and did not consider the dose from an internal criticality. Although the Zircaloy cladding is resistant to direct attack by nitric acid, cladding destabilization may occur allowing the buildup of metal-halide complexes in solutions that can promote corrosion (CRWMS M&O 2000b, p. II–1). Screening arguments for this corrosion mechanism show that environments conducive to the accumulation of the necessary chemical species are unlikely.

The U.S. Nuclear Regulatory Commission (NRC) has also expressed a concern during key technical information exchanges regarding the effects on criticality consequence evaluations resulting from radiation from the criticality event (Reamer and Williams 2000, p. 6). In particular, their concern is that although Zircaloy has excellent corrosion resistance to nitric acid and hydrogen peroxide, the concentration of these species can be enhanced by radiolysis during an internal WP criticality, potentially accelerating the corrosion effects in the cladding material.

Attachment III contains the text of the white paper responding to the NRC/DOE (U.S. Department of Energy) DOE Criticality Key Technical Issue regarding radiolytic enhancement of Zircaloy corrosion rates resulting from an internal WP criticality. The white paper documented a scoping calculation of the radiolytic generation potential for nitric acid and an estimate of the consequences with respect to corrosion rates of Zircaloy. The chemical environment conducive to enhanced corrosion rates was identified and compared with possible conditions resulting from a static criticality. Based upon the scoping calculation results, radiolytic contributions to enhanced corrosion rates from criticality events could not be screened out from consideration. Mitigating effects from the chemical interactions, however, may reduce possibilities for accelerated Zircaloy corrosion. A detailed geochemical calculation of such factors was outside the scope of the initial calculation. It should be noted, however, that the radiolytic production rate of nitric acid during a static criticality event from the detailed calculation (Section 6 of this document) is within 10% of the rate from the scoping calculation (Attachment III). Thus, consequences relating to accelerated corrosion rates for Zircaloy derived from the detailed geochemistry calculation are not expected to differ significantly from the scoping calculation, i.e., a potential exists for lowering the pH of the WP environment but scavenging effects may prevent sufficient accumulation of nitric acid to affect corrosion rates.

The purpose of this calculation is to provide a detailed calculation the potential for generation of radiolytic species during a postulated static criticality event in a WP. The consequences of any radiolytic specie generation, estimated in Attachment III, will be addressed in a revision to this calculation.

This calculation is done in accordance with the *Technical Work Plan for: Waste Package Design Description for LA* (License Application) (BSC [Bechtel SAIC Company] 2001a, Section 3). Details of this activity are in Section 3, Tasks for Work Scope 2, Disposal Criticality Analysis Methodology Development. The work plan calls for resolution of all items in the revised DCTR for which NRC acceptance is sought. The calculational method, input description, and results from this calculation are given in the following sections.

2. METHOD

Radiolytic production of particular chemical species depends upon the radiation environment, the chemical components present, and the physical environment where the radiolytic reactions are occurring. However, the yield of any given chemical species is characterized by a single parameter, "G", identified as the G-factor (Reed and Van Konynenburg 1991, pp. 1396-1403). The "G" value represents the number of molecules of a chemical species produced per 100 eV of absorbed radiation energy in the volume containing the irradiated environment. Measurements of the "G" factor for production of nitrogen dioxide (one-to-one production ratio for nitric acid) from mixed neutron-gamma radiation range from approximately 0.5 to 2.5 molecules/100 eV of absorbed energy (Reed and Van Konynenburg 1991, p. 1399). The value used in this calculation is 1.0 (Assumption 3.3) and this value is also assumed to apply to neutron irradiation (Assumption 3.3). The acid production rate scales linearly with the "G" factor and the uncertainty in the factor expressed in Section 6 as range of possible molar quantities of nitric acid generated. The "G" value of 1.0 was chosen for this calculation to be consistent with other radiolytic acid production calculations discussed in Section 5.

For this calculation, a 21-pressurized water reactor (PWR) WP, containing commercial spent nuclear fuel (CSNF) assemblies, was assumed to have failed and subsequently partially filled with water. The steel basket structure was assumed to have fully degraded with the degradation products settling to the bottom of the WP. Hematite (Fe_2O_3) is assumed to be the only iron-bearing degradation product formed from the original basket material (Assumption 3.1). This is consistent with previous studies (CRWMS M&O 1997, Section 7.1.1) that showed that replacement of hematite by goethite had little effect on criticality. In a separate suite of evaluations, the contribution to the degradation product volume from diaspore generated by oxidized aluminum from the thermal shunt plates is also considered. The packing fraction of the hematite, or the hematite-diaspore mixture, was assumed to be 0.58 (Assumption 3.2), with the remaining space filled with water. For evaluations involving mixtures, complete reaction of the Fe and Al in the donating structures provides a mole fraction of 0.8439 (mass fraction = 0.9350) for the hematite in the degradation product mixture material. Degradation products were assumed to be present outside the fuel pins in assemblies below the degradation product-water mixture level, but not within the guide tube and instrument tube spaces of those assemblies. The water level above the degradation product-water mixture was assumed to extend sufficiently high to maintain criticality, leaving an air-water vapor space at the top of the WP. The radiant energy deposition in the air-water vapor space was calculated with the MCNP code (Briesmeister, 1997) using the KCODE option and tracking the transport of both neutron and gamma particles. The gamma interactions include photon and electron processes leading to dissociation of the gas molecules and generation of nitric acids in the air-water vapor space.

A KCODE calculation provides the combined estimates (track length, collision, and absorption) of k_{eff} for the waste package (Briesmeister 1997, p. 2-153). Additionally, the code collects information about events that occur during the calculation in set of variables known as tallies. A series of these tallies have been specified in the MCNP input decks to obtain estimates for the following physical quantities:

1. Total, neutron, and gamma energy depositions, in MeV, in the moist air regions of the waste package
2. Average energy released per fission for the waste package
3. Average number of neutrons released per fission for the waste package
4. k_{eff} for each of the SNF regions: the fuel pins surrounded by degradation products (lower region), the fuel pins surrounded by water (middle region), and the fuel pins surrounded by moist air (top region) (see Figure 5.4 for region definition).

Information is collected for both gamma and neutron events using "f6" and "f4" tally types that are defined as

f6 energy deposition averaged over a cell in MeV/g
f4 flux averaged over a cell in particles/cm^2.

The MCNP results for the specified tallies are provided per fission neutron.

2.1 ENERGY DEPOSITION

The combination of the "f6" tally card and an "sd" segment divisor card that sets the mass divisors of the cells to unity provides the track length estimate of cell energy deposition, in MeV. The cell energy deposition is the integral over the cell volume, time range, and particle energy range from the total reaction rate in the cell multiplied by the heating response, as shown in Equation 1 (Briesmeister 1997, p. 2-72)

$$ED = \rho_a \int_V \int_t \int_E \sigma_T(E)\Phi(\vec{r}, E, t)H(E)dEdtdV \qquad \text{Eq. 1}$$

where:

ED = energy deposition (MeV)
ρ_a = atom density (atoms/barn-cm)
$\sigma_T(E)$ = total microscopic cross-section (barn)
$\Phi(\vec{r}, E, t)$ = particle flux (neutrons or photons/cm^{2}s)
H(E) = heating response (MeV)
V = cell volume (cm^3)
E = neutron or photon energy (MeV)
t = time (s).

The f6 tally is equivalent to a f4 track length estimate of cell flux modified by energy-dependent multipliers, which consist of the particle total reaction rate number and the heating number on a fm card (tally multiplier, Briesmeister 1997, p. 2-73). The reaction numbers used as multipliers are –1 (total cross section) and –4 (average heating number) for neutrons and –5 (total cross section) and –6 (photon heating number) for photons (Briesmeister 1997, p. 3-77). This equivalent tally has been specified in the MCNP calculations for verification purposes.

2.2 TRACK LENGTH ESTIMATOR FOR k_{eff}

The track length estimator for k_{eff} provides an estimate for the integral shown in Equation 2. This estimator has been specified in the MCNP input using an "f4:n" (neutron) tally card, an "fm" card that contains the –6 (total fission cross section) and –7 (number of neutrons released per fission) reaction multipliers, and an "sd" card (volume multiplier) that sets the fuel region volume to unity (Briesmeister 1997, pp. 2-151 and 2-163) given by

$$k_{eff} = \rho_a \int_{V\,t\,E} \Phi(\vec{r}, E, t)\,dE\,dt\,dV \sum_k f_k \bar{\nu}_k(E)\sigma_{fk}(E) \qquad \text{Eq. 2}$$

where:

f_k = atomic fraction for nuclide k
$\sigma_{fk}(E)$ = microscopic neutron fission cross section (barn) for nuclide k
$\bar{\nu}_k(E)$ = average number of prompt or total neutrons produced per fission by the collision nuclide at the incident neutron energy.

2.3 AVERAGE NUMBER OF NEUTRONS RELEASED PER FISSION

The average number of neutrons released per fission for the system is calculated as the ratio of total neutrons released in fission events to the fission reaction rate, as shown in Equation 3

$$\nu_{avg} = \frac{\rho_a \int_{V\,t\,E} \Phi(\vec{r}, E, t)\,dE\,dt\,dV \sum_k f_k \bar{\nu}_k(E)\sigma_{fk}(E)}{\rho_a \int_{V\,t\,E} \sigma_f(E)\Phi(\vec{r}, E, t)\,dE\,dt\,dV} \qquad \text{Eq. 3}$$

where:

$\sigma_f(E)$ = total microscopic fission cross-section (barn).

The numerator of the fraction is evaluated using the track length estimator for k_{eff}, as described in the previous section. The f4 tally (track length estimator for cell flux) and the –6 multiplier provide an estimate for the total fission reaction rate, which represents the denominator of the fraction.

2.4 AVERAGE ENERGY RELEASED PER FISSION

The average energy released per fission is calculated using the ratio of the estimated total fission energy released to the fission reaction rate, as shown in Equation 4

$$Q_{avg} = \frac{\rho_a \int_{V\,t\,E} \Phi(\vec{r}, E, t)\,dE\,dt\,dV \sum_k f_k \sigma_{fk}(E)\bar{Q}_k(E)}{\rho_a \int_{V\,t\,E} \sigma_f(E)\Phi(\vec{r}, E, t)\,dE\,dt\,dV} \qquad \text{Eq. 4}$$

where:

Q_{avg} = average energy released per fission (MeV/fission)
$Q_k(E)$ = average energy produced per fission by the collision nuclide at the incident neutron energy.

The numerator of the fraction is evaluated using the f4 tally and the –6 and –8 (fission energy) multiplier. The denominator is evaluated as described in the previous section.

Control of the electronic management of data is accomplished in accordance with the process control evaluation for technical work plan of this calculation (BSC 2001a).

3. ASSUMPTIONS

3.1 It is assumed that the steel in the basket assembly and fuel assembly end fittings is fully degraded. Hematite (Fe_2O_3) and Diaspore (ALO(OH)) are assumed to be the only degradation products remaining from the steel internals. The rational for this assumption is that these minerals have a very low solubility whereas other degradation products with higher solubilities are more likely to be transported out of the WP. This minimizes the amount of neutron absorber materials in the WP which is conservative. This assumption is used in Sections 2 and 5.

3.2 It is assumed that the porosity of packed particles resulting from degradation of the steel and aluminum internal structure of a 21 PWR WP is 42%. The rationale for this assumption is that measurements of the porosity of compacted granular materials (sand) was limited to approximately 42% before onset of container distortion (CRWMS M&O 1998b, p. 15). This assumption is used in Sections 2, 5, and 6.

3.3 It is assumed that the "G" factor for radiolytic production of nitric acid has the same value for neutron radiation as for gamma radiation. The rationale for this assumption is that radiolytic specie production is proportional to the absorbed energy rather than the effective dose. This assumption is used in Sections 2, 5, and 6.

3.4 It is assumed that the spacing between fuel assemblies in an asymmetric arrangement (resting on the WP) is 0.25 cm. The rationale for this assumption is that degradation products from the basket structure remaining between assemblies will prevent direct contact between assemblies This assumption is used in Sections 5 and 6.

3.5 It is assumed that the stainless steel inner shell of the WP is not degraded. The rationale for this assumption is that it is conservative. Degradation products from the WP shell would increase the total volume of the hematite in the WP, thus decreasing the moist air space available for radiolytic reactions. This assumption is used in Sections 5 and 6.

3.6 It is assumed that the Babcock and Wilcox (B&W) Mark B 15x15 fuel design used for this calculation is representative of the fuel types anticipated for potential disposition in the MGR. The basis for this assumption is this assembly type has been used for WP source term (CRWMS M&O 1999a, Section 3) and radiolysis calculations (BSC 2001b, Section 5.2). This assumption is used in Section 5.

3.7 It is assumed that the instrument tube in a B&W Mark B fuel assembly is the same length as the fuel pins. The rationale for this assumption is that it is conservative allowing slightly more moderator within the assemblies immersed in the degradation products. This assumption is used in Section 5.

4. USE OF COMPUTER SOFTWARE AND MODELS

4.1 COMPUTER SOFTWARE

4.1.1 MCNP

The MCNP code (CRWMS M&O 1998c), qualified according to Office of Civilian Radioactive Waste Management (OCRWM) procedure AP-SI.1Q, *Software Management*, was used to calculate the effective neutron multiplication factor (k_{eff}) of the system and radiant energy deposition in the vapor space of the WP. The software specifications are as follows:

- Software name: MCNP
- Software version/revision number: Version 4B2
- Software tracking number (CSCI): 30033 V4B2LV
- Computer type: Hewlett Packard (HP) 9000 Series Workstations
- Computer processing unit number: Software is installed on the CRWMS M&O workstation "bloom" whose CRWMS M&O Tag number is 700887.

The input and output files for the various MCNP calculations are contained on a compact disk-read only memory (CD-ROM) (Attachment II) with the files documented in Attachment I. The calculation spreadsheets described in Sections 5 and 6 and included in Attachment II are such that an independent repetition of the calculations may be performed.

The MCNP software used was:

(a) appropriate for the calculation of criticality and radiant energy deposition (MCNP is a Monte Carlo computer program designed for criticality calculations and for tracking neutron and gamma radiation)

(b) used only within the range of validation (benchmark cases used in validation the code include a number of critical configurations involving UO_2 fuels and shielding configurations involving neutron and gamma particle transport CRWMS M&O 1998a)

(c) obtained from the Software Configuration Management in accordance with appropriate procedures.

4.1.2 Excel

- Title: Excel
- Version/Revision Number: Microsoft® Excel 97 SR-2
- This software is installed on a personal computer running Microsoft Windows 95 with CRWMS M&O Tag number 113136.

Microsoft Excel for Windows, Version 97 SR-2, was used in this calculation to translate the input data into the correct format and units using standard mathematical expressions and operations. It was also used to reformulate and display results. The user-defined formulas, inputs, and results are documented in sufficient detail to allow an independent repetition of computations. Thus, Microsoft Excel is used only as a worksheet and not as a software routine. Microsoft Excel is an exempt software product according to OCRWM procedure AP-SI.1Q, *Software Management*.

4.2 MODELS

None used.

5. CALCULATION

As stated in Section 1, the purpose of this calculation is to evaluate the potential for production of radiolytic nitric acid during a postulated criticality event involving intact PWR CSNF in a degraded basket configuration inside a 21-PWR WP. The PWR CSNF used in the calculation were B&W 15x15 PWR assemblies (Assumption 3.6) having a five wt% initial ^{235}U enrichment, 30 GWd/MTU (GigaWatt-days/metric ton uranium) burnup, and a 25,000 year radionuclide decay period.

The reference design for the repository (CRWMS M&O 2000a, Section 1.7.1) features a line loading of WPs, a drip shield with no backfill, emplacement of the WPs on a corrosion resistant pallet with a nominal spacing of ten centimeters between WPs, resting on an invert filled with crushed tuff. The principal components of this design are illustrated by the drift segment shown in Figure 5.1. The 21-PWR WP configuration that is the basis for MCNP representation used in this calculation is illustrated in Figure 5.2. Descriptions of the MCNP representation of the WP, fuel assemblies, and other data used in the calculation are given in the following sections.

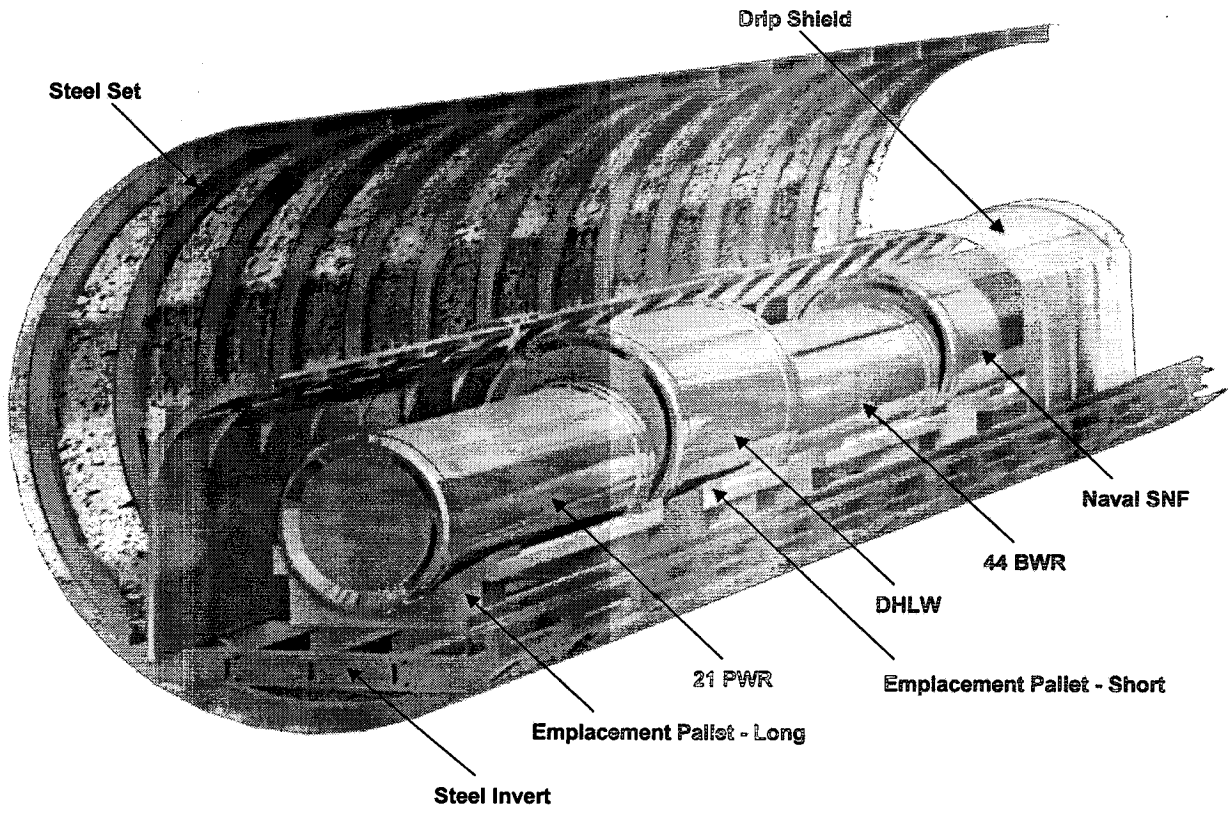

Figure 5.1. MGR Drift Segment Showing Waste Packages, Pallets, and Drip Shield

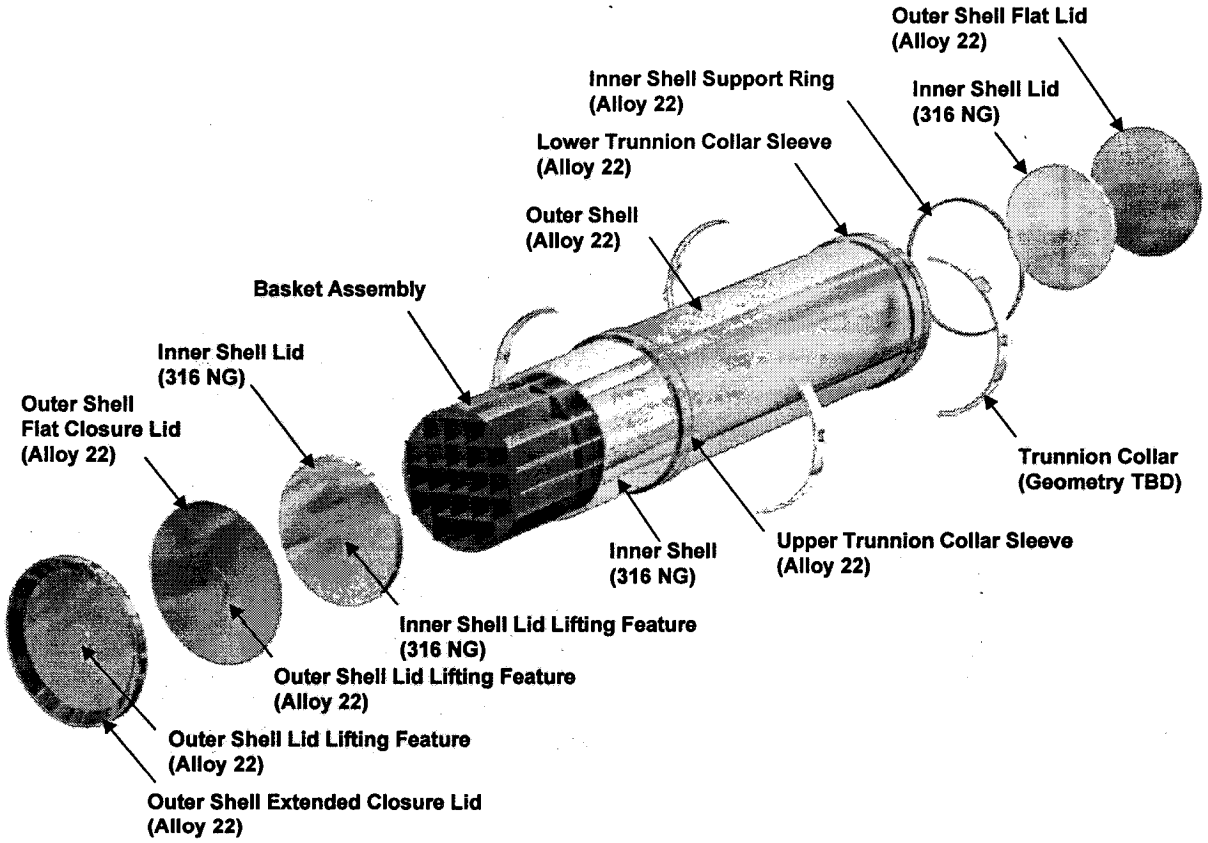

Figure 5.2. 21-PWR Waste Package Assembly Configuration

5.1 LIST AND STATUS OF INPUT DATASETS

The document tracking numbers (DTN) used in this calculation are listed in Table 5.1. These DTNs are all qualified-verification level 2, for uses not supporting the principal factors.

Table 5.1. Summary List of Input DTNs

Input	Content
DTN: MO0003RIB00071.000	Physical and Chemical Characteristics of Alloy 22
DTN: MO0003RIB00076.000	Physical and Chemical Characteristics of Type 316N Grade Stainless Steel
DTN: MO9906RIB00048.000	Waste Package Material Properties: Waste Form Materials
DTN: MO9906RIB00054.000	Waste Package Material Properties: Structural Materials

5.2 INPUT DESCRIPTION

5.2.1 21-PWR Waste Package

The 21-PWR WP, illustrated in Figure 5.2, consists of an inner shell of 316 NG stainless steel for strength, an outer shell of corrosion resistant Alloy 22, inner shell lids of 316 NG stainless steel, outer shell lids of Alloy 22, and the basket assembly of 516 carbon steel containing embedded Neutronite absorber plates. The WP geometry and dimensions of the WP are listed in Table 5.2. For this calculation, the basket assembly is assumed to be fully degraded (Assumption 3.1). Products resulting from the degradation of the basket are assumed to be in a settled configuration which is the most reactive configuration. Gross CSNF assembly (DOE 1987, p. 2A-31 – 2A-45) and WP component (CRWMS M&O 2000e, Attachment I) masses and materials are listed in Table 5.3.

Table 5.2. Waste Package Dimensions

Parameter	Value	Units	Radius	Basis
Inner Shell OD	152.4	cm	76.2	CRWMS M&O 2000e, Attachment I
Inner Shell ID	142.4	cm	71.2	CRWMS M&O 2000e, Attachment I
Inner Shell Length	477.5	cm	-	CRWMS M&O 2000e, Attachment I
Inner Shell Lid Diameter	142.0	cm	71.0	CRWMS M&O 2000e, Attachment I
Inner Shell Lid Thickness	9.5	cm	-	CRWMS M&O 2000e, Attachment I
Outer Shell OD	156.4	cm	78.2	CRWMS M&O 2000e, Attachment I
Outer Shell ID	152.4	cm	76.2	CRWMS M&O 2000e, Attachment I
Outer Shell Length	501.5	cm	-	CRWMS M&O 2000e, Attachment I
Outer Shell Lid Diameter	152.7	cm	76.35	CRWMS M&O 2000e, Attachment I
Outer Shell Lid Thickness	1.0 (top flat) 2.5 (base and extension)	cm	-	CRWMS M&O 2000e, Attachment I
Total Waste Package Length	516.5	cm	-	CRWMS M&O 2000e, Attachment I
Inner Shell Cavity Volume	$7.30212 \cdot 10^6$	cm^3	-	inner shell dimension data in this table

Table 5.3. Components and Material Inventories for Waste Package

Components	Mass (kg)	Material	Basis
Outer WP Shell and Lids	4880	Alloy 22	CRWMS M&O 2000e, Attachment I
Inner WP Shell and Lids	11109	Stainless Steel 316	CRWMS M&O 2000e, Attachment I
Basket Tubes, Sideguides, Cornerguides and Stiffeners	5723.68	A 516 Carbon Steel Grade 70	CRWMS M&O 2000e, Attachment I
Fuel Basket Plates A, B and C	2064	Neutronit A 978	CRWMS M&O 2000e, Attachment I
Fuel Basket Plates D and E	336	SB 209 Aluminum 6061	CRWMS M&O 2000e, Attachment I
Assembly Nozzle – Top (/assbly)	7.480	Stainless Steel CF3M	DOE 1987, p. 2A-32
Assembly Nozzle – Bottom (/assbly)	8.160	Stainless Steel CF3M	DOE 1987, p. 2A-32
Assembly Spring Retainer (/assbly)	0.910	Stainless Steel CF3M	DOE 1987, p. 2A-32
Assembly Upper End Plugs (/assbly)	0.060	Stainless Steel 304	DOE 1987, p. 2A-32
Assembly Lower Nuts (/assbly)	0.150	Stainless Steel 304	DOE 1987, p. 2A-32
Assembly Upper Nuts (/assbly)	0.510	Stainless Steel 304L	DOE 1987, p. 2A-32
Assembly Spacer – Plenum (/assbly)	1.040	Inconel 718	DOE 1987, p. 2A-32
Assembly Spacer – Bottom (/assbly)	1.300	Inconel 718	DOE 1987, p. 2A-32
Assembly Spacers – Core (/assbly)	4.900	Inconel 718	DOE 1987, p. 2A-32
Holddown Spring (/assbly)	1.800	Inconel 718	DOE 1987, p. 2A-32
Assembly Instrument Tube (/assbly)	0.640	Zircaloy 4	DOE 1987, p. 2A-32
Assembly Guide Tubes (/assbly)	8.000	Zircaloy 4	DOE 1987, p. 2A-32

5.2.2 B&W Mark B Intact Fuel Assembly

The representations of the B&W 15x15 Mark B PWR fuel assembly in the calculations use nominal specifications and parameters (DOE 1987, p. 2A-32 – 2A-35 and Punatar 2001, p. 2-4 – 2-10). Intact assembly specifications and dimensions are provided in Table 5.4. Assembly dimensions are given primarily in English units and converted into metric units. The number of digits in the corresponding metric value column is a result of the direct units conversion and is not indicative of precision. These parameters are used as input to the degradation product inventory calculations (see Attachment II), the MCNP k_{eff} searches, and collision density calculations (Attachment II). The initial assembly heavy metal (i.e., U) inventory specified in Table 5.4 differs by less than 3% from the value used for definition of the fuel composition (CRWMS M&O 1999a, p. 23, Table 12) used for calculating the 30 GWd/MTU burnup and 25,000 year decay isotopic of the fuel assemblies, and is therefore acceptable for use in these calculations of system mass and volume (Attachment II). The WP shell dimensions (CRWMS M&O 2000e, Attachment I) given in Table 5.2 are also input to the calculations as necessary.

Table 5.4. Mechanical Parameters of the B&W 15x15 Mark B Fuel Assembly

Parameter	Value	Units	Metric	Units	Radius	Basis
Fuel Rods	208	/assbly	208	/assbly	-	DOE 1987, p. 2A-33 and 2A-45
Fuel Rod Positions on an Assembly Side	15	/side	15	/side	-	Punatar 2001, p. 2-5, Table 2-2
Guide Tubes	16	/assbly	16	/assbly	-	DOE 1987, p. 2A-32 and 2A-44
Instrumentation Tubes	1	/assbly	1	/assbly	-	DOE 1987, p. 2A-32 and 2A-44
Total Guide + Instrument Tubes	17	/assbly	17	/assbly	-	sum of guide and instrument tubes
Clad, Guide and Instrument Tube Material	Zircalloy-4		Zircalloy-4		-	Punatar 2001, p. 2-5, Table 2-2
Fuel Pellet OD[a]	0.3686	in	0.936244	cm	0.468122	Punatar 2001, p. 2-5, Table 2-2
Active Fuel Rod Length	141.8	in	360.172	cm	-	Punatar 2001, p. 2-5, Table 2-2
Total Fuel Rod Length	153.687	in	390.366	cm	-	Punatar 2001, p. 2-15
Fuel Clad OD	0.430	in	1.0922	cm	0.5461	Punatar 2001, p. 2-5, Table 2-2
Clad Wall Thickness	0.0265	in	0.06731	cm	-	DOE 1987, p. 2A-33 and 2A-45
Fuel Clad ID[a]	0.377	in	0.95758	cm	0.47879	Punatar 2001, p. 2-5, Table 2-2
Fuel Clad End Cap Thickness	0.2811	in	0.714	cm	-	Punatar 2001, p. 2-15
Fuel Rod Pitch	0.568	in	1.44272	cm	-	Punatar 2001, p. 2-5, Table 2-2
Guide Tube OD	0.530	in	1.3462	cm	0.6731	Punatar 2001, p. 2-10
Guide Tube Wall Thickness	0.016	in	0.04064	cm	-	difference between outer and inner radii
Guide Tube ID	0.498	in	1.26492	cm	0.63246	Punatar 2001, p. 2-10
Guide Tube Length	156.313	in	397.035	cm	-	Punatar 2001, p. 2-10
Instrument Tube OD	0.544067	in	1.38193	cm	0.69097	Punatar 2001, p. 2-10
Instrument Tube Wall Thickness	0.051534	in	0.13090	cm	-	Difference between outer and inner radii
Instrument Tube ID	0.4410	in	1.12014	cm	0.56007	Punatar 2001, p. 2-10
Instrument Tube Length	153.5	in	389.890	cm	-	Punatar 2001, p. 2-10
Fuel Assembly Height	165.625	in	420.6875	cm	-	DOE 1987, p. 2A-31 and 2A-43
Mass of U	1022.12	lbm /assbly	463.63	kg /assbly	-	DOE 1987, p. 2A-31 and 2A-43

Parameter	Value	Units	Metric	Units	Radius	Basis
Fuel Assembly Width	8.536	in	21.68144	cm	-	DOE 1987, p. 2A-31 and 2A-43
Fuel Assembly Pitch	9.6693(sym) 8.6344(asym)	in	24.560(sym) 21.93144(asym)	cm	-	Assumption
Fuel Assembly Volumetric Displacement	$5.2297 \cdot 10^3$	in^3	$8.570 \cdot 10^4$	cm^3	-	Assembly pin, guide and instrument tube data in this table

NOTE: Table 5.3 entries do not reflect significant digits where necessitated by unit conversions.
[a] OD (outside diameter), ID (inside diameter)

5.2.3 Material Compositions and Density

Material compositions and mass densities used in number density and degradation product volume calculations are listed in Table 5.5. The Neutronit A 978 composition used in calculations neglects the 2.2 (wt %) Mo, with assignment of the Mo content to Fe. The isotope ^{95}Mo is a principal isotope (YMP 2000, p. 3-34, Table 3-3) that has a natural abundance of 15.92 (atom %) and a ground state thermal neutron capture cross section of 110 (b) (Parrington et al. 1996, p. 31). The neglect of Mo in the basket plates contributes to conservative assessment from a neutronic standpoint, as the Mo does not contribute to parasitic neutron capture.

Table 5.5. Material Specification for the Waste Package Container and Fuel Hardware

A 516 Carbon Steel Grade 70						
Mass Density (kg/m^3)						Basis
7850						ASME[a] 1998, Section II-A, SA-20, p. 67
Composition (wt %)						Basis
Carbon (max)	0.27	Manganese	1.025	Phosphorus (max)	0.035	ASME 1998, Section II-A, SA-516, p. 925
Silicon	0.275	Sulfur (max)	0.035	Iron (balance)	98.36	

Stainless Steel CF3M						
Mass Density (kg/m^3)						Basis
8000						SS 316N mass density from DTN: MO0003RIB00076.000
Composition (wt %)						Basis
Carbon (max)	0.03	Chromium	19.0	Manganese (max)	1.5	SAE 1993, p. 141. Additional 2.5 (wt %) Mo, with equivalent reduction for Fe, incorporated in mass balance.
Molybdenum	2.5	Nickel	11.0	Phosphorus (max)	0.04	
Silicon (max)	1.50	Sulfur (max)	0.04	Iron (balance)	64.39	

Stainless Steel 302						
Mass Density (kg/m^3)						Basis
7940						SS 304 mass density from DTN: MO9906RIB00054.000
Composition (wt %)						Basis
Carbon (max)	0.15	Chromium	18.0	Manganese (max)	2.0	SAE 1993, p. 251
Nickel	9.0	Phosphorus (max)	0.045	Sulfur (max)	0.03	
Silicon (max)	1.0	Iron (balance)	69.775			

Stainless Steel 304						
Mass Density (kg/m^3)						Basis
7940						DTN: MO9906RIB00054.000
Composition (wt %)						Basis
Carbon (max)	0.08	Chromium	19.0	Manganese (max)	2.0	DTN: MO9906RIB00054.000
Nickel	9.25	Nitrogen (max)	0.1	Phosphorus (max)	0.045	
Sulfur (max)	0.03	Silicon (max)	1.0	Iron (balance)	68.495	

Stainless Steel 304L						
Mass Density (kg/m^3)						Basis
7940						DTN: MO9906RIB00054.000
Composition (wt %)						Basis
Carbon (max)	0.03	Chromium	19.0	Manganese (max)	2.0	DTN: MO9906RIB00054.000
Nickel	10.0	Nitrogen	0.1	Phosphorus (max)	0.045	
Sulfur (max)	0.03	Silicon (max)	0.75	Iron (balance)	68.045	

Stainless Steel 316						
Mass Density (kg/m^3)						Basis
7980						SS 316L mass density from DTN: MO9906RIB00054.000
Composition (wt %)						Basis
Carbon (max)	0.08	Chromium	17.00	Manganese (max)	2.00	ASME 1998, Section II-A, SA-240, p. 366
Molybdenum	2.50	Nickel	12.00	Phosphorus (max)	0.045	
Silicon (max)	0.75	Sulfur (max)	0.03	Nitrogen (max)	0.10	
Iron (balance)	65.495					

Neutronit A 978						
Mass Density (kg/m^3)						Basis
7760						Kugler 1996, p. 17
Composition (wt %)						Basis
Boron (min)	0.75	Carbon (max)	0.04	Chromium	18.5	Kugler 1996, p. 14 and ASTM A887-89, p. 2
Cobalt (max)	0.2	Nickel	13.0	Iron (balance)	67.51	

Alloy 22						
Mass Density (kg/m^3)						Basis
8690						DTN: MO0003RIB00071.000
Composition (wt %)						Basis
Carbon (max)	0.015	Chromium	21.25	Cobalt (max)	2.5	DTN: MO0003RIB00071.000
Iron	4.0	Manganese (max)	0.5	Molybdenum	13.5	
Phosphorus (max)	0.02	Silicon (max)	0.08	Sulfur (max)	0.02	
Tungsten (max)	3.0	Vanadium (max)	0.35	Nickel (balance)	54.765	

Inconel 718						
Mass Density (kg/m^3)						Basis
8190						DTN: MO9906RIB00054.000
Composition (wt %)						Basis
Aluminum	0.5	Carbon	0.04	Chromium	19.0	DTN: MO9906RIB00054.000
Columbium	5.13	Manganese	0.18	Molybdenum	3.05	
Nickel	52.5	Silicon	0.18	Sulfur	0.008	
Titanium	0.9	Iron (balance)	18.512			

Zircaloy 4						
Mass Density (kg/m^3)						Basis
6560						DTN: MO9906RIB00048.000
Composition (wt %)						Basis
Chromium	0.1	Iron	0.21	Oxygen	0.125	DTN: MO9906RIB00048.000
Tin	1.45	Zirconium (balance)	98.115			

SB 209 Aluminum 6061						
Mass Density (kg/m^3)						Basis
2700						DTN: MO9906RIB00048.000
Composition (wt %)						Basis
Chromium	0.195	Copper	0.275	Iron (max)	0.7	DTN: MO9906RIB00048.000
Manganese (max)	0.15	Magnesium	1.0	Silicon	0.6	
Titanium (max)	0.15	Zinc (max)	0.25	Aluminum (balance)	96.68	

NOTE: Minor differences exist between the compositional specifications for Stainless Steel 302, Stainless Steel 316 and Neutronit A 978 in Table 5.5 and in the mass balance calculations (Attachment II, File "21-PWR-EDAII-A-0914_cor.xls", Sheet "Vol-Mass"). These compositional specifications have no effect on the degradation product compositions, because neither the plenum spring nor inner WP shell materials are degraded in the assessments.
[a] American Society of Mechanical Engineers.

Isotopic and elemental atomic weights are given in Table 5.6. Table 5.7 defines the CSNF composition for a nominal LEU PWR assembly with an initial fissile enrichment of 5.0 (wt %), 30 GWd/MTU burnup, and 25,000 years of post-irradiation isotopic decay (CRWMS M&O 1999b, Disk 3, File "Waste.Stream.E2.R1.B7.cut", TBV-4111). This combination of high initial enrichment and relatively low burnup is not representative of the average assembly in the PWR commercial waste stream, and is conservative because it contributes to a high reactivity attribute. The assembly definition taken for the source term calculation uses an initial heavy

metal inventory of 475 kg (CRWMS M&O 1999a, p. 23, Table 12) , which differs from the specification in Table 5.3 by less than 3%. The isotopic inventories specified in Table 5.7 are based on the assembly definition of CRWMS M&O 1999a (p. 23, Table 12).

Table 5.6. Isotopic and Atomic Weights

Isotope or Element	Atomic Weight (amu) or (g/mole)	Basis
H	1.00794	Parrington et al. 1996, p. 62
O	15.9994	Parrington et al. 1996, p. 63
Al	26.981538	Parrington et al. 1996, p. 63
Fe	55.845	Parrington et al. 1996, p. 62
^{95}Mo	94.905841	Parrington et al. 1996, p. 31
^{99}Tc	98.9062545	Audi and Wapstra 1995, p. 22
^{101}Ru	100.905581	Parrington et al. 1996, p. 31
^{103}Rh	102.905504	Parrington et al. 1996, p. 31
^{109}Ag	108.904756	Parrington et al. 1996, p. 31
^{143}Nd	142.909810	Parrington et al. 1996, p. 37
^{145}Nd	144.912569	Parrington et al. 1996, p. 37
^{147}Sm	146.914894	Parrington et al. 1996, p. 36
^{149}Sm	148.917180	Parrington et al. 1996, p. 36
^{150}Sm	149.917272	Parrington et al. 1996, p. 36
^{152}Sm	151.919729	Parrington et al. 1996, p. 36
^{151}Eu	150.919846	Parrington et al. 1996, p. 36
^{153}Eu	152.921226	Parrington et al. 1996, p. 36
^{155}Gd	154.922619	Parrington et al. 1996, p. 36
^{233}U	233.039627	Parrington et al. 1996, p. 49
^{234}U	234.040945	Parrington et al. 1996, p. 49
^{235}U	235.043922	Parrington et al. 1996, p. 49
^{236}U	236.045561	Parrington et al. 1996, p. 48
^{238}U	238.050785	Parrington et al. 1996, p. 48
^{237}Np	237.048166	Parrington et al. 1996, p. 48
^{239}Pu	239.052156	Parrington et al. 1996, p. 48
^{240}Pu	240.053808	Parrington et al. 1996, p. 48
^{241}Pu	241.056845	Audi and Wapstra 1995, p. 61
^{242}Pu	242.058737	Parrington et al. 1996, p. 48
^{241}Am	241.056822	Parrington et al. 1996, p. 48
^{243}Am	243.061374	Parrington et al. 1996, p. 48

Table 5.7. CSNF Composition

Isotope	Mass (g/assbly)	Number Density $(b \cdot cm)^{-1}$
^{16}O[a]	6.39E+04	4.6628E-02
^{95}Mo	3.52E+02	4.3307E-05
^{99}Tc	3.29E+02	3.8840E-05
^{101}Ru	3.31E+02	3.8302E-05
^{103}Rh	2.07E+02	2.3488E-05
^{109}Ag	2.72E+01	2.9163E-06
^{143}Nd	4.20E+02	3.4316E-05
^{145}Nd	3.14E+02	2.5301E-05
^{147}Sm	1.33E+02	1.0570E-05
^{149}Sm	2.10E+00	1.6466E-07
^{150}Sm	1.32E+02	1.0281E-05
^{152}Sm	5.52E+01	4.2426E-06
^{151}Eu	9.29E+00	7.1875E-07
^{153}Eu	4.22E+01	3.2222E-06
^{155}Gd	1.79E+00	1.3491E-07
^{233}U	5.08E+00	2.5453E-07
^{234}U	1.82E+02	9.0801E-06
^{235}U	1.21E+04	6.0110E-04
^{236}U	3.24E+03	1.6027E-04
^{238}U	4.43E+05	2.1729E-02
^{237}Np	6.82E+02	3.3594E-05
^{239}Pu	1.40E+03	6.8382E-05
^{240}Pu	5.80E+01	2.8212E-06
^{241}Pu	1.98E-05	9.5908E-13
^{242}Pu	1.00E+02	4.8238E-06
^{241}Am	5.97E-04	2.8918E-11
^{243}Am	1.58E+00	7.5902E-08

NOTE: data in Table 5.7 use exponential notation: e.g., $1.0 \cdot 10^{-3}$ = 1.0E-03
isotopic mass inventories from CRWMS M&O 1999b, Disk 3, File "Waste.Stream.E2.R1.B7.cut"
[a] ^{16}O mass inventory satisfies UO_2 composition. see Attachment II, File "fuel_comp.xls", sheet "25,000"

5.2.4 Degradation Product Inventories

Degradation product inventories and characteristics are summarized in Table 5.8. Calculations for the hematite and diaspore volumes and masses are made in Attachment II, File "21-PWR-EDAII-A-0914_cor.xls", Sheet "Vol-Mass", assuming a 58% solid volume fraction in the degradation product mixture. The 58% solid volume fraction is derived from compacted granular material and represents an upper bound on the solid fraction (Assumption 3.2). Degradation product volumes and masses are converted to number densities in Attachment II, File "deg_comp.xls", Sheet "Number_Densities."

Table 5.8. Degradation Product Inventories and Characteristics

Hematite Only			
Solid Product Volume Fraction (%)	Mixture Mass Density[a,b] (g/cm^3)		Volume[b] (cm^3)
58	3.4592		3.4209E+06
Fe Density[c] $(b \cdot cm)^{-1}$	Al Density[c] $(b \cdot cm)^{-1}$	O Density[c] $(b \cdot cm)^{-1}$	H Density[c] $(b \cdot cm)^{-1}$
2.29228E-02	0.00000E+00	4.84239E-02	2.80795E-02
Configuration	Degradation Product Mixture Height[d] (cm)		Water Level Height[d] (cm)
Symmetric	13.62160		36.2
Asymmetric	19.90699		71.2

Hematite and Diaspore			
Solid Product Volume Fraction (%)	Mixture Mass Density[a,b] (g/cm^3)		Volume[b] (cm^3)
58	3.3899		3.7871E+06
Fe Density[c] $(b \cdot cm)^{-1}$	Al Density[c] $(b \cdot cm)^{-1}$	O Density[c] $(b \cdot cm)^{-1}$	H Density[c] $(b \cdot cm)^{-1}$
2.14338E-02	1.28589E-03	4.87622E-02	2.93654E-02
Configuration	Degradation Product Mixture Height[d] (cm)		Water Level Height[d] (cm)
Symmetric	22.02201		47.0
Asymmetric	27.95594		N/A

NOTE: some data in Table 5.8 use exponential notation: e.g., $1.0 \cdot 10^{-3}$ = 1.0E-03
[a] nominal water density of 1.0 (g/cc), see Table 6.1
[b] see Attachment II, File "21-PWR-EDAII-A-0914_cor.xls", Sheet "Vol-Mass"
[c] see Attachment II, File "deg_comp.xls", Sheet "Number_Densities"
[d] height from WP axis elevation.

5.3 MCNP REPRESENTATION OF 21-PWR WASTE PACKAGE

A principal assumption for this calculation (Assumption 3.1) is that the steel components (basket assembly and fuel assembly end fitting) are completely degraded with only the Hematite and (optionally) Diaspore remaining in the WP. The fuel assemblies, with Zircaloy cladding and spacer grids, remain intact. The MCNP representation of the assemblies is thus limited to the fuel pins, guide tubes, and instrument tubes. The assembly descriptions consist of four axial zones, partially disjoint, that are based upon the fuel composition distribution. One zone includes the fuel pin end caps and spacers, the second zone includes the gas plenums and springs, the third zone contains the active fuel region, and the last zone contains only the guide tubes which extend beyond the fuel pins. This configuration is illustrated in Figure 5.3.

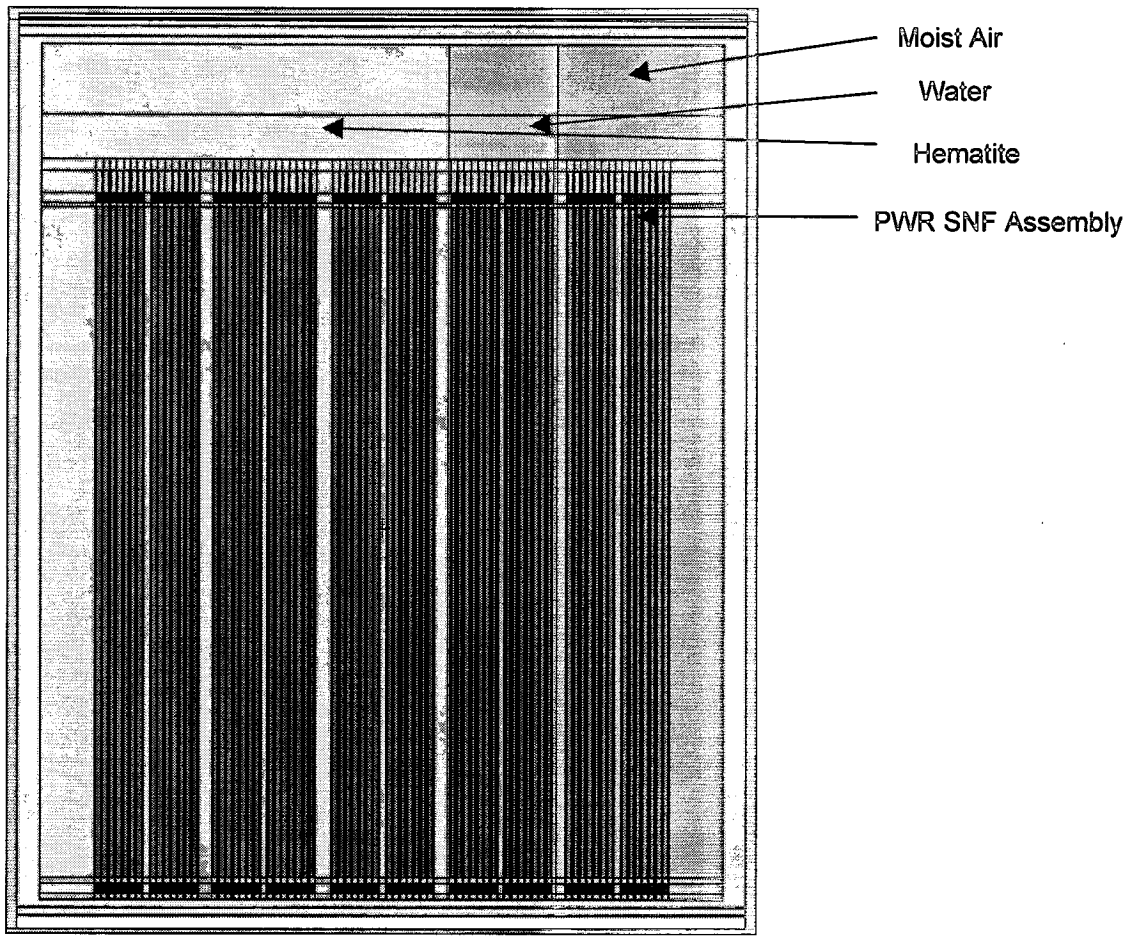

NOTE: Drawing not to scale.

Figure 5.3. Waste Package Vertical Cross Section

At the time of original repository emplacement, the CSNF assemblies occupy the basket bays illustrated in Figure 5.2. Two MCNP representations of the 21-PWR WP and fuel assemblies were constructed, one configuration having a symmetric crosssectional arrangement of fuel assemblies and the second with an asymmetric arrangement. These representations are illustrated in Figures 5.4 and 5.5, respectively. The symmetric configuration is very conservative with respect to the criticality potential of the WP.

Configurational subclasses were defined for the radiolysis calculations based on the maintenance of the original assembly spacing with respect to the package horizontal crossectional plane. In the symmetric case (Figure 5.3), the original relative assembly spacing was maintained, averaging 24.56 cm for the assembly pitch throughout the basket structure, despite basket plate, thermal shunt and fuel tube degradation. The absolute assembly locations are frozen at the original design positions allowing no vertical or horizontal displacements, with

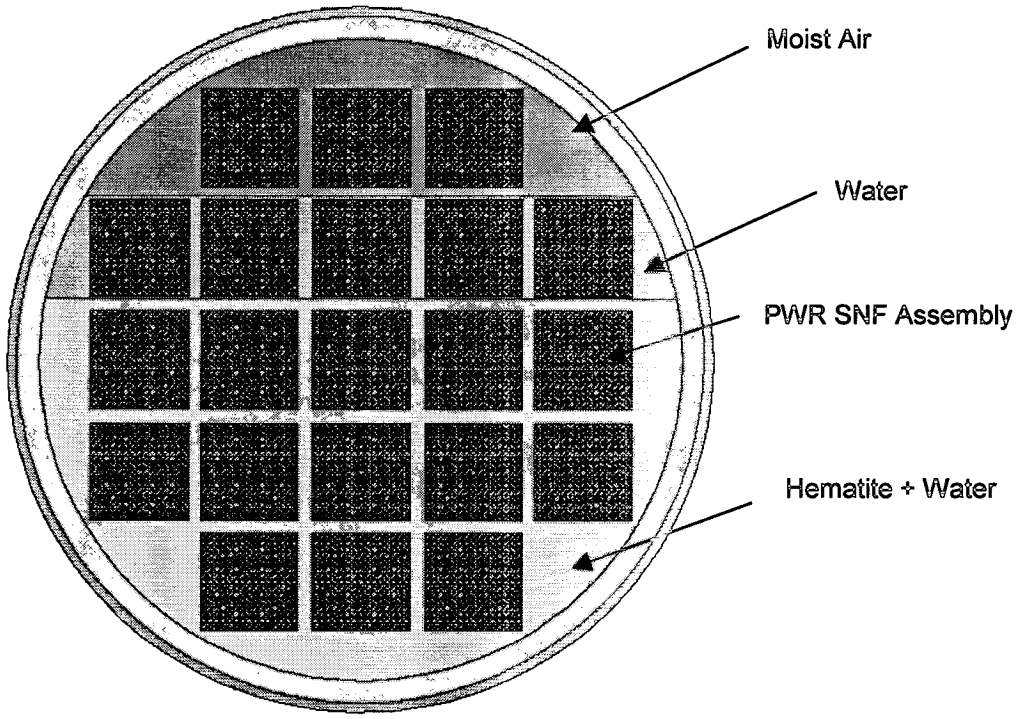

Figure 5.4. Symmetric Configuration: Hematite Degradation Product

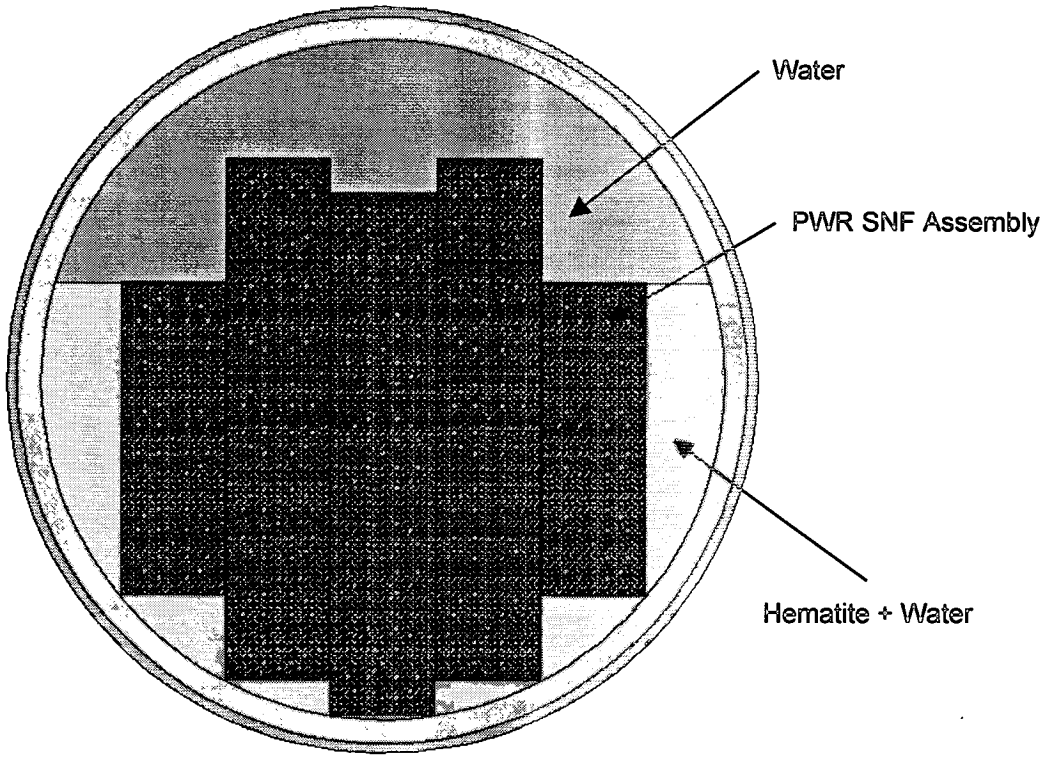

Figure 5.5. Asymmetric Configuration: Hematite Degradation Product

the degradation product mixture occupying the assembly interstices and the available waste package cavity void space. Degradation products were excluded from the interior of the guide tubes and instrument tubes since, in the horizontal position, there is little likelihood these products will enter the tubes. The maintenance of original assembly positions is a bounding configuration for the determination of k_{eff} because it maximizes the fraction of CSNF assemblies residing above the degradation product mixture line, thereby placing more assemblies in an overlying water moderated region and maximizing the assembly multiplication worths.

The asymmetric configuration (Figure 5.5) accounts for the vertical settling of the assemblies within the WP cavity. The assembly pitch is the assembly width plus a 0.250-cm interstitial separation (Assumption 3.4). Vertical translations of the assemblies from the original positions create five columns of assemblies, with the lowest row of assemblies contacting the surface at the base of the inner WP shell. The resulting spatial distribution of assemblies is asymmetric with respect to the WP cross-section, but still symmetric with respect to the bi-lateral arrangement. The hematite and diaspore degradation product mixture occupies the assembly interstices and the accessible WP cavity void space excluding the assembly guide tubes and instrument tubes.

Configurational subclasses were identified according to assumptions concerning the degradation products remaining in the WP. If all of the steel and aluminum structures within the WP, excluding the shell and closure lids, and exposed assembly hardware are degraded, the hematite displacement volume exceeds the diaspore displacement volume by approximately a factor of 10 (see Attachment II, File "21-PWR-EDAII-A-0914_cor.xls", Sheet "Vol-Mass"). The degradation product mixture definition is varied parametrically to determine the influence of including or excluding the minor Al-bearing fraction of the mixture. In combination with variations for symmetric or asymmetric configurations, parametric variations produce a total of four distinct degraded configurations:

1. symmetric assembly configuration, with hematite only
2. symmetric assembly configuration, with hematite and diaspore
3. asymmetric assembly configuration, with hematite only
4. asymmetric assembly configuration, with hematite and diaspore.

The configurations with Hematite as the only degradation product are illustrated in Figure 5.4 for the symmetric case and Figure 5.5 for the asymmetric case. The symmetric configuration with both Hematite and Diaspore as degradation products is illustrated in Figure 5.6. These figures also show the crosssectional areas occupied by the degradation product mixture, water, and moist air. For the asymmetric configuration, criticality could not be achieved with any moist air space in the WP (Section 6) , and thus radiolytic specie production can not occur for that configuration.

The energy deposition in the air filled region calculated by MCNP is given in units of MeV per fission neutron. This energy must be multiplied by nubar (number of neutrons per fission) and number of fission events occurring in a criticality to obtain the total energy deposition from a

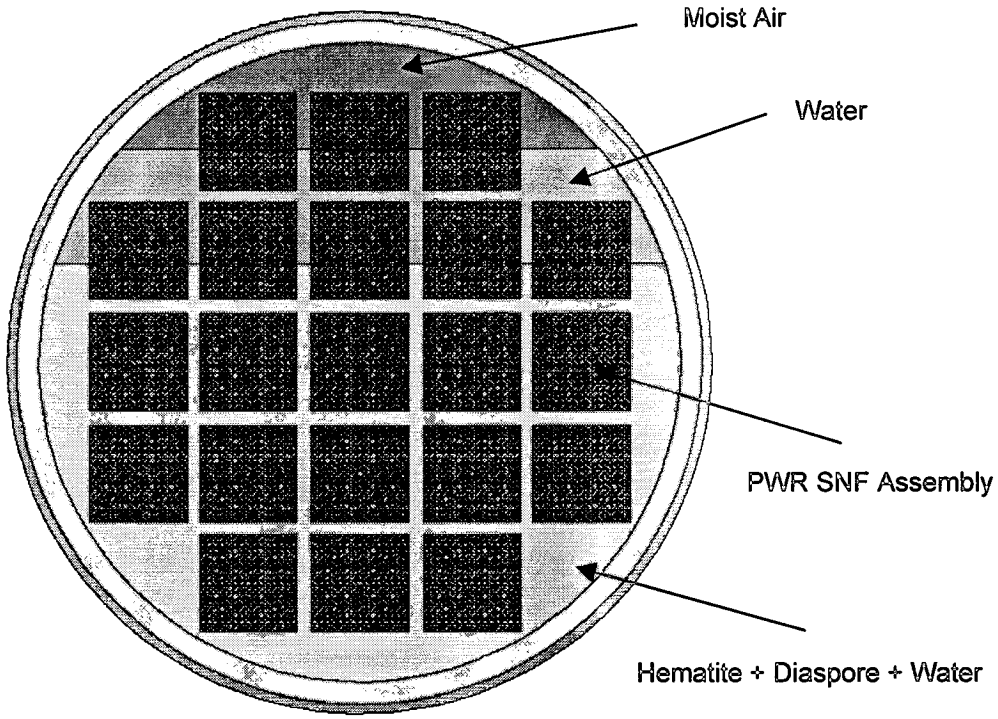

Figure 5.6. Symmetric Configuration: Hematite and Diaspore Degradation Products

postulated criticality. These operations are documented in the spreadsheet file "21-PWR-EDAII-A-0914_cor.xls" (sheet "Tally-result") included in Attachment II.

6. RESULTS

This document may be affected by technical product input information that requires confirmation. Any changes to the document that may occur as a result of completing the confirmation activities will be reflected in subsequent revisions. The status of the technical product input information quality may be confirmed by review of the Document Input Reference System database (AP-3.15Q, *Managing Technical Product Inputs.* Section 5.4.1e).

As stated in Section 1, radiolytic specie generation that has any potential for enhancing corrosion rates within a WP requires a critical configuration operating over some period of time. In addition, there must be a void space in the WP containing air and water vapor, sources for the radiolytic radicals that ultimately combing to form nitric acid. Thus the WP configurations identified in Section 5 were screened for having a criticality potential coupled with a void space. The level of the degradation product mixture was fixed since its volume was known and the critical water level above the mixture then determined iteratively. These levels, as given in Table 6.1, are 36.2 cm and 47.0 cm for the symmetric configuration with Hematite only and Hematite plus Diaspore, respectively. The asymmetric configuration was near criticality with Hematite only but the water level at the top of the WP leaving no space for radiolytic specie production. With both Hematite and Diaspore as degradation products in the asymmetric configuration, criticality was not possible. The degradation product mixture level, critical water level, and MCNP tally quantities described in Section 2 are summarized in Table 6.1.

The radiant energy deposition, in MeV per fission neutron, in the WP regions filled with moist air for the symmetric configurations are listed in Table 6.2 for the Hematite degradation product case and for the Hematite plus Diaspore case in Table 6.3. The tallies were summed over all of the void locations in the WP with the numbered locations identified in Figure 6.1. It should be noted that regions numbered from two through five consist of the union of lattice all assemblies in the void region.

The radiolytic production of nitric acid for a static criticality averaging one kW is given in Table 6.1 as 7.41E-03 moles/year/kW with Hematite only as the degradation product and 4.07E-3 moles/year/kW with both Hematite and Diaspore as degradation products (Spreadsheet "21-PWR-EDAII-A-0914_cor.xls ", Sheet "Tally-result", Row 162-171). As stated in Section 2, the "G" factor for nitric acid production ranges from 0.5 to 2.5. The "G" value used in deriving the quoted production rate was 1.0 but the results scale linearly with the "G" value. The production rates also scale linearly with time in years and the criticality power level in kW.

Table 6.1. Critical Configuration Parameters

	Waste Package Configuration			
	Symmetric-Hematite	Symmetric-Hematite + Diaspore	Asymmetric-Hematite	Asymmetric-Hematite + Diaspore
Hematite Level[a] (cm)	13.62160	N/A[c]	19.90699	N/A
Hematite + Diaspore Level	N/A	22.02201	N/A	27.95594
Water Level for the Critical Configuration[a] (cm)	36.20	47.00	71.2	N/A
k_{eff} for the Waste Package Lower Region[b]	0.2217±0.0010	0.2799±0.0011	0.3789±0.0013	0.5881±0.0015
k_{eff} for the Waste Package Middle Region[b]	0.7289+0.0019	0.6846±0.0018	0.6157±0.0017	0.3401±0.0014
k_{eff} for the Waste Package Top Region[b]	0.0494±0.0004	0.0350±0.0004	N/A	N/A
Track Length Estimator for k_{eff}	1.0000±0.0018	0.9995±0.0018	0.9946±0.0017	0.9281±0.0017
Combined Estimator for k_{eff}	0.9995±0.0011	1.0009±0.0011	0.9945±0.0012	0.9285±0.0011
Average Number of Neutrons Released per Fission	2.5361±0.0091	2.5344±0.0091	N/A	N/A
Average Energy Released per Fission (MeV)	182.3374±0.6564	182.3296±0.6564	N/A	N/A
Nitric Acid Production Rate[d] Moles/year/kW	7.41E-03	4.07E-03	N/A	N/A

NOTES: [a] The levels of degradation products and water from the waste package center
[b] Track length estimator for k_{eff}
[c] Not applicable
[d] "21-PWR-EDAII-A-0914_cor.xls" (sheet "Tally-result")

The specie production rate scales as the number of fissions per unit interval and, thus, linearly for steady-state events. For a one kW average static criticality event extending over 10,000 years (maximum steady state duration assumed for consequence analyses), approximately 74 moles or 4.7 kg of HNO_3 could possibly be produced, assuming a "G" factor of 1.0. Uncertainty in the "G" factor results in a range of approximately 37 to 185 moles for the total acid production from such a hypothetical static criticality event.

The 74-mole quantity of HNO_3 from the hypothetical static criticality calculation compares to approximately 20moles of HNO_3 produced over 90,000 years at < 4 rad/hr from radionuclide decay (BSC 2001b, Section 6).

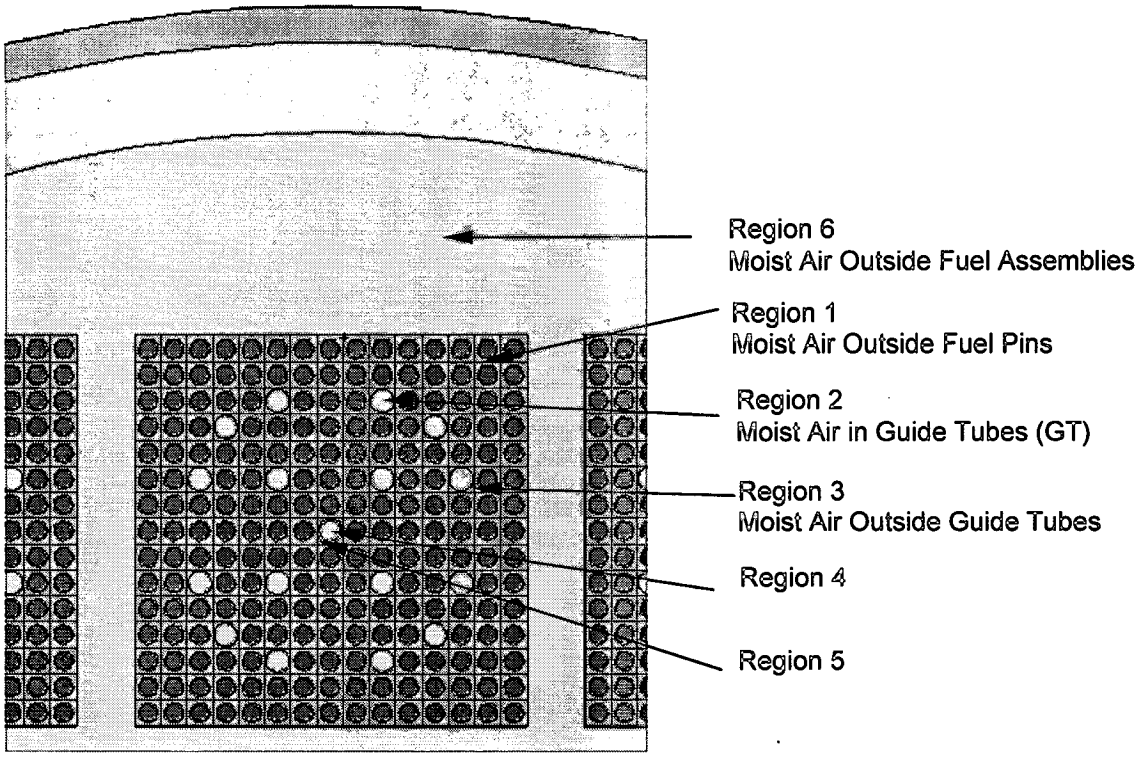

Figure 6.1. Tally Regions in MCNP Calculations

Table 6.2. Energy Deposition for the Symmetric Configuration with Hematite as the Degradation Product

Moist Air Region		Total		Neutron		Gamma	
Axial Location	Radial Location	ED (MeV/neutron)	Relative Error	ED (MeV/neutron)	Relative Error	ED (MeV/neutron)	Relative Error
Fuel pin end caps and spacers	1	3.40E-07	0.0230	2.10E-07	0.0245	1.30E-07	0.0422
	2	2.83E-08	0.0426	1.83E-08	0.0420	1.01E-08	0.0913
	3	1.45E-08	0.0382	9.38E-09	0.0397	5.12E-09	0.0776
	4	1.13E-09	0.1646	7.04E-10	0.1670	4.26E-10	0.3361
	5	5.90E-10	0.1222	4.08E-10	0.1338	1.82E-10	0.2568
	6	8.63E-07	0.0210	4.42E-07	0.0212	4.21E-07	0.0349
Fuel pin gas plenums	1	2.63E-07	0.0275	1.53E-07	0.0264	1.10E-07	0.0532
	2	2.03E-08	0.0476	1.21E-08	0.0479	8.20E-09	0.0930
	3	1.02E-08	0.0428	6.39E-09	0.0440	3.76E-09	0.0870
	4	1.03E-09	0.1952	6.35E-10	0.2281	3.90E-10	0.3539
	5	5.92E-10	0.1335	3.87E-10	0.1330	2.04E-10	0.2923

Moist Air Region	Total	Neutron	Gamma				
Axial Location	Radial Location	ED (MeV/neutron)	Relative Error	ED (MeV/neutron)	Relative Error	ED (MeV/neutron)	Relative Error
	6	6.10E-07	0.0222	3.11E-07	0.0225	2.99E-07	0.0368
Active fuel	1	4.90E-05	0.0031	3.06E-05	0.0036	1.84E-05	0.0049
	2	3.90E-06	0.0047	2.55E-06	0.0049	1.35E-06	0.0092
	3	2.04E-06	0.0045	1.33E-06	0.0047	7.06E-07	0.0088
	4	1.80E-07	0.0152	1.25E-07	0.0151	5.46E-08	0.0352
	5	1.05E-07	0.0129	7.38E-08	0.0131	3.14E-08	0.0295
	6	1.03E-04	0.0033	5.44E-05	0.0036	4.87E-05	0.0053
GT zone without fuel pins	Lattice cells other than GT cells	1.22E-07	0.0467	6.83E-08	0.0472	5.37E-08	0.0842
	2	4.89E-09	0.0915	3.09E-09	0.0962	1.80E-09	0.1812
	3	2.88E-09	0.0859	1.83E-09	0.0989	1.05E-09	0.1574
	Outside assemblies	1.88E-07	0.0438	9.34E-08	0.0415	9.48E-08	0.0731
Top end fittings	Entire	9.11E-07	0.0369	4.01E-07	0.0375	5.09E-07	0.0541
Above assemblies	Entire	8.92E-07	0.0429	3.71E-07	0.0457	5.21E-07	0.0601
Total		1.63E-04	0.0029	9.12E-05	0.0033	7.14E-05	0.0045

Table 6.3. Energy Deposition for the Symmetric Configuration with Hematite and Diaspore as Degradation Products

Moist Air Region		**Total**		**Neutron**		**Gamma**	
Axial Location	**Radial Location**	**ED (MeV/neutron)**	**Relative Error**	**ED (MeV/neutron)**	**Relative Error**	**ED (MeV/neutron)**	**Relative Error**
Fuel pin end caps and spacers	1	2.25E-07	0.0270	1.30E-07	0.0302	9.52E-08	0.0457
	2	1.53E-08	0.0544	9.51E-09	0.0604	5.75E-09	0.1028
	3	8.09E-09	0.0523	4.89E-09	0.0607	3.20E-09	0.0925
	4	1.46E-09	0.1352	7.29E-10	0.1363	7.28E-10	0.2336
	5	8.31E-10	0.1088	5.04E-10	0.1315	3.27E-10	0.1878
	6	5.36E-07	0.0263	2.67E-07	0.0271	2.69E-07	0.0425
Fuel pin gas plenums	1	1.80E-07	0.0305	9.63E-08	0.0316	8.37E-08	0.0526
	2	1.14E-08	0.0613	6.53E-09	0.0664	4.92E-09	0.1109
	3	5.83E-09	0.0534	3.40E-09	0.0600	2.43E-09	0.0953
	4	1.66E-09	0.1440	1.10E-09	0.1784	5.52E-10	0.2437
	5	6.93E-10	0.1197	4.07E-10	0.1327	2.86E-10	0.2158
	6	3.85E-07	0.0277	1.91E-07	0.0293	1.94E-07	0.0447
Active fuel	1	3.19E-05	0.0035	1.83E-05	0.0041	1.35E-05	0.0054
	2	2.04E-06	0.0060	1.24E-06	0.0064	7.93E-07	0.0112
	3	1.11E-06	0.0056	6.69E-07	0.0060	4.38E-07	0.0103
	4	2.76E-07	0.0137	1.53E-07	0.0140	1.23E-07	0.0250
	5	1.63E-07	0.0122	8.95E-08	0.0122	7.37E-08	0.0223
	6	5.17E-05	0.0044	2.72E-05	0.0049	2.45E-05	0.0068

Moist Air Region		Total		Neutron		Gamma	
Axial Location	**Radial Location**	**ED (MeV/neutron)**	**Relative Error**	**ED (MeV/neutron)**	**Relative Error**	**ED (MeV/neutron)**	**Relative Error**
GT zone without fuel pins	Lattice cells other than GT cells	6.86E-08	0.0586	3.64E-08	0.0622	3.22E-08	0.0984
	2	2.99E-09	0.1185	1.67E-09	0.1378	1.31E-09	0.2041
	3	1.39E-09	0.1060	7.33E-10	0.1191	6.61E-10	0.1799
	Outside assemblies	1.21E-07	0.0540	4.77E-08	0.0567	7.28E-08	0.0768
Top end fittings	Entire	4.62E-07	0.0476	1.97E-07	0.0476	2.66E-07	0.0695
Above assemblies	Entire	3.67E-07	0.0576	1.48E-07	0.0616	2.19E-07	0.0798
Total		8.95E-05	0.0036	4.89E-05	0.0041	4.06E-05	0.0054

7. REFERENCES

7.1 DOCUMENTS CITED

Audi, G. and Wapstra, A.H. 1995. *Atomic Mass Adjustment, Mass List for Analysis.* [Upton, New York: Brookhaven National Laboratory, National Nuclear Data Center]. TIC: 242718.

BSC (Bechtel SAIC Company) 2001a. *Technical Work Plan for: Waste Package Design Description for LA.* TWP-EBS-MD-000004 REV 01. Las Vegas, Nevada: Bechtel SAIC Company. ACC: MOL.20010702.0152.

BSC (Bechtel SAIC Company) 2001b. *Gamma and Neutron Radiolysis in the 21-PWR Waste Package.* CAL-MGR-NU-000006 REV 00. Las Vegas, Nevada: Bechtel SAIC Company. ACC: MOL.20010522.0198.

Briesmeister, J.F., ed. 1997. *MCNP-A General Monte Carlo N-Particle Transport Code.* LA-12625-M, Version 4B. Los Alamos, New Mexico: Los Alamos National Laboratory. ACC: MOL.19980624.0328.

CRWMS M&O 1997. *Criticality Evaluation of Degraded Internal Configurations for the PWR AUCF WP Designs.* BBA000000-01717-0200-00056 REV 00. Las Vegas, Nevada: CRWMS M&O. ACC: MOL.19971231.0251.

CRWMS M&O 1998a. *Software Qualification Report for MCNP Version 4B2, A General Monte Carlo N-Particle Transport Code.* CSCI: 30033 V4B2LV. DI: 30033-2003 Rev. 01. Las Vegas, Nevada: CRWMS M&O. ACC: MOL.19980622.0637.

CRWMS M&O 1998b. *Supplemental Criticality Evaluation for Degraded Internal Configurations of a 21 PWR Waste Package.* BBA000000-01717-0210-00022 REV 00. Las Vegas, Nevada: CRWMS M&O. ACC: MOL.19980918.0086.

CRWMS M&O 1998c. *Software Code: MCNP.* 4B2LV. HP. 30033 V4B2LV.

CRWMS M&O 1999a. *PWR Source Term Generation and Evaluation.* BBAC00000-01717-0210-00010 REV 01. Las Vegas, Nevada: CRWMS M&O. ACC: MOL.20000113.0333.

CRWMS M&O 1999b. *Output Files for PWR Source Term Generation and Evaluation.* BBAC00000-01717-0210-00010 REV 01. Las Vegas, Nevada: CRWMS M&O. ACC: MOL.19991111.0702.

CRWMS M&O 2000a. *Total System Performance Assessment for the Site Recommendation.* TDR-WIS-PA-000001 REV 00 ICN 01. Las Vegas, Nevada: CRWMS M&O. ACC: MOL.20001220.0045.

CRWMS M&O 2000b. *Summary of In-Package Chemistry for Waste Forms.* ANL-EBS-MD-000050 REV 01. Las Vegas, Nevada: CRWMS M&O. ACC: MOL.20010129.0134.

CRWMS M&O 2000c. *Waste Form Degradation Process Model Report.* TDR-WIS-MD-000001 REV 00 ICN 01. Las Vegas, Nevada: CRWMS M&O. ACC: MOL. 20000713.0362.

CRWMS M&O 2000d. *Clad Degradation - FEPs Screening Arguments.* ANL-WIS-MD-000008 REV 00 ICN 01. Las Vegas, Nevada. CRWMS M&O. ACC: MOL.20001208.0061.

CRWMS M&O 2000e. *Design Analysis for UCF Waste Packages.* ANL-UDC-MD-000001 REV 00. Las Vegas, Nevada: CRWMS M&O. ACC: MOL.20000526.0336.

CRWMS M&O 2001a. *FEPs Screening of Processes and Issues in Drip Shield and Waste Package Degradation.* ANL-EBS-PA-000002 REV 01. Las Vegas, Nevada: CRWMS M&O. ACC: MOL.2000216.0004.

DOE (U.S. Department of Energy) 1987. *Appendix 2A, Physical Descriptions of LWR Fuel Assemblies.* Volume 3 of *Characteristics of Spent Fuel, High-Level Waste, and Other Radioactive Waste Which May Require Long-Term Isolation.* DOE/RW-0184. Washington, D.C.: U.S. Department of Energy, Office of Civilian Radioactive Waste Management. ACC: HQX.19880405.0024.

Kugler, A. 1996. *Bohler Neutronit A976 Sheet and Plate for Nuclear Engineering.* Murzzuschlag, Austria: Bohler Bleche GmbH. TIC: 240558.

Parrington, J.R.; Knox, H.D.; Breneman, S.L.; Baum, E.M.; and Feiner, F. 1996. *Nuclides and Isotopes, Chart of the Nuclides.* 15th Edition. San Jose, California: General Electric Company and KAPL, Inc.. TIC: 233705.

Punatar, M.K. 2001. *Summary Report of Commercial Reactor Criticality Data for Crystal River Unit 3.* TDR-UDC-NU-000001 REV 02. Las Vegas, Nevada: Bechtel SAIC Company. ACC: MOL.20010702.0087.

Reamer, C.W. and Williams, D.R. 2000. Summary Highlights of NRC/DOE Technical Exchange and Management Meeting on Subissues Related to Criticality. Meeting held October 23-24, 2000, Las Vegas, Nevada. Washington, D.C.: U.S. Nuclear Regulatory Commission. ACC: MOL.20001208.0097 through MOL.20001208.0110.

Reed, D.T. and Van Konynenburg, R.A. 1988. "Effect of Ionizing Radiation on Moist Air Systems." *Scientific Basis for Nuclear Waste Management XI, Symposium held November 30-December 3, 1987, Boston, Massachusetts, USA.* Apted, M.J. and Westerman, R.E., eds. *112,* 393-404. Pittsburgh, Pennsylvania: Materials Research Society. TIC: 203662.

Reed, D.T. and Van Konynenburg, R.A. 1991. "Effect of Ionizing Radiation on the Waste Package Environment." *High Level Radioactive Waste Management, Proceedings of the Second*

Annual International Conference, Las Vegas, Nevada, April 28-May 3, 1991. 2, 1396-1403. La Grange Park, Illinois: American Nuclear Society. TIC: 204272.

Shoesmith, D.W. and King, F. 1998. *The Effects of Gamma Radiation on the Corrosion of Candidate Materials for the Fabrication of Nuclear Waste Packages.* AECL-11999. Pinawa, Manitoba, Canada: Atomic Energy of Canada Limited. ACC: MOL.19990311.0212.

YMP (Yucca Mountain Site Characterization Project) 2000. *Disposal Criticality Analysis Methodology Topical Report.* YMP/TR-004Q, Rev. 01. Las Vegas, Nevada: Yucca Mountain Site Characterization Office. ACC: MOL.20001214.0001.

7.2 INPUT DATA BY DATA TRACKING NUMBER

MO0003RIB00071.000. Physical and Chemical Characteristics of Alloy 22. Submittal Date: 03/13/2000.

MO0003RIB00076.000. Physical and Chemical Characteristics of Type 316N Grade. Submittal Date: 03/14/2000.

MO9906RIB00048.000. Waste Package Material Properties: Waste Form Materials. Submittal Date: 6/9/1999.

MO9906RIB00054.000. Waste Package Material Properties: Structural Materials. Submittal Date: 06/17/1999.

7.3 CODES, STANDARDS, REGULATIONS, AND PROCEDURES

AP-3.12Q, Rev. 0, ICN 4. *Calculations.* Washington, D.C.: U.S. Department of Energy, Office of Civilian Radioactive Waste Management. ACC: MOL.20010404.0008.

AP-3.15Q, Rev. 3. *Managing Technical Product Inputs.* Washington, D.C.: U.S. Department of Energy, Office of Civilian Radioactive Waste Management. ACC: MOL.20010801.0318.

AP-SI.1Q, Rev. 3, ICN 1, ECN 1. *Software Management.* Washington, D.C.: U.S. Department of Energy, Office of Civilian Radioactive Waste Management. ACC: MOL.20010705.0239.

ASME (American Society of Mechanical Engineers) 1998. *1998 ASME Boiler and Pressure Vessel Code.* 1998 Edition with 1999 and 2000 Addenda. New York, New York: American Society of Mechanical Engineers. TIC: 247429.

ASTM A 887-89. 1992. *Standard Specification for Borated Stainless Steel Plate, Sheet, and Strip for Nuclear Application.* Philadelphia, Pennsylvania: ASTM. TIC: 245311.

SAE 1993. *Metals & Alloys in the Unified Numbering System.* 6th Edition. Warrendale, Pennsylvania: Society of Automotive Engineers. TIC: 243414.

ATTACHMENTS

A list of attachments to this calculation is provided below.

I. List of files on CD-ROM (Attachment II).

II. CD-ROM with data files for calculation.

III. White paper documenting the initial scoping calculation.

ATTACHMENT I

The Excel spreadsheets and MCNP input and output files are provided on a compact disk and are listed in Table I.1. Each file is identified by its name, size (in bytes), and the date and time of last access. It should be noted that for files transferred from the HP workstation to the personal computer, the date and time reflect the time of transfer. The actual date and time of run completion can be found in the file.

Table I.1. File Attributes for the Contents of Attachment II

File Name	Description	File Size (bytes)	File Date	File Time
a-h.i	MCNP input file for the asymmetric configuration with hematite degradation product	46,938	09/24/2001	4:02 p.m.
a-h.io	MCNP output file for the asymmetric configuration with hematite degradation product	1,311,887	09/24/2001	4:02 p.m.
a-hd.i	MCNP input file for the asymmetric configuration with hematite and diaspore degradation products	46,896	09/24/2001	4:02 p.m.
a_hd.io	MCNP output file for the asymmetric configuration with hematite and diaspore degradation products	1,318,225	09/24/2001	4:02 p.m.
s-h.i	MCNP input file for the symmetric configuration with hematite degradation product	49,077	09/24/2001	9:56 a.m.
s-h.io	MCNP output file for the symmetric configuration with hematite degradation product	1,691,217	09/24/2001	9:56 a.m.
s_hd.i	MCNP input file for the symmetric configuration with hematite and diaspore degradation products	49,075	09/24/2001	4:02 p.m.
s_hd.io	MCNP output file for the symmetric configuration with hematite and diaspore degradation products	1,729,002	09/24/2001	4:02 p.m.
fuel_comp.xls	Spreadsheet to calculate fuel atom densities	19,456	09/26/2001	1:39 p.m.
deg_comp.xls	Spreadsheet to calculate degradation product number densities	22,016	09/24/2001	9:33 a.m.
21-PWR-EDAII-A-0914_cor.xls	Spreadsheets to calculate WP and fuel assembly geometry, composition, critical water height, number densities, and radiolytic specie production	286,208	09/27/2001	3:56 p.m.

ATTACHMENT II

Attachment II is a CD-ROM containing the files listed in Attachment I.

ATTACHMENT III

Attachment III contains the text of the white paper documenting the initial scoping calculation of the potential for radiolytic generation of nitric acid during a static criticality in a CSNF WP and estimation of the consequences of such production with respect to possible corrosion enhancement of Zircaloy cladding.

Summary

Accelerated corrosion rates due to radiolytic chemical specie generation (primarily nitric acid) have been considered in the repository degradation models and, for the most part, eliminated from further consideration due to the low specie generation from radionuclide decay. However, the radiation dose from a criticality event may generate significantly greater quantities of nitric acid than from radionuclide decay that could result in a low pH within the WP. A low pH, coupled with an increase in fluoride concentration, could accelerate cladding corrosion rates.

A scoping calculation performed to estimate the range of possible quantities that could be generated from an internal waste package steady-state criticality resulted in 40-200 moles. This amount of nitric acid could result in low pH values (< 2) in the WP. This estimate does not account for possible mitigating reactions, such as with the Hematite, that scavenge the nitric acid. Calculations with EQ6 are proposed to investigate the effects on the evolution of the chemical environment in the WP when nitric acid is added to the mixture.

Scoping Calculation of Potential for Enhanced Corrosion in a 21 PWR Waste Package from Chemical Species Generated by Radiolysis Effects during a Criticality Event

January 19, 2001

I. Introduction

The effects of radiation on the corrosion of various metals and alloys, particularly with respect to in-reactor processes, has been discussed by a number of authors (Shoesmith and King 1999, p. 1). Shoesmith and King (1999) additionally discuss the effects of radiation on proposed Monitored Geologic Repository (MGR) Waste Package (WP) materials. Radiation effects on the corrosion of metals and alloys include, among other things, radiolysis of the local gaseous and aqueous environment to produce oxidizing and reducing radicals. In particular, radiolysis processes in moist air environments lead to the fixation of nitrogen as NO, NO_2, and especially HNO_3 (Reed and Van Konynenburg 1988, pp. 393-404). The nitric acid is produced in an irradiated air-water vapor system when the hydroxyl radicals generated from the water vapor convert nitrogen dioxides, which are formed by the radiolytic reaction between nitrogen and oxygen, to nitric acids.

Chemical species produced by radiolysis have been identified as a mechanism for accelerating corrosion of the MGR engineered barrier system (EBS), in the Disposal Criticality Analysis Methodology Topical Report (DCTR) (CRWMS M&O 2000a, p. 2-2). Radiolytic sources of corrosion have also been considered in the screening of processes and issues in the drip shield and WP degradation (CRWMS M&O 2000b, Section 6.2.27), Yucca Mountain Project (YMP) FEP (features, events, and processes) No. 2.1.13.01.00. The latter reference dealt specifically with radiolytic effects of gamma radiation on the WP and drip shield, excluding them from

further consideration because of low consequence. The potential for chemical interactions within the WP from radiolytic effects was considered insignificant in the Waste Form Degradation Process Model Report (CRWMS M&O 2000c, p. 3-21) and therefore neglected except as a possible perforation mechanism for the Zircaloy cladding (CRWMS M&O 2000c, p. 3-40). The rationale is that although Zircaloy has excellent corrosion resistance to nitric acid and hydrogen peroxide, the concentration of these species can be enhanced by radiolysis during an internal waste package criticality, potentially accelerating the corrosion effects in the cladding material.

Radiolysis producing local depression of pH resulting in localized corrosion of cladding material is included in the localized corrosion model as a special feature, YMP FEP NO. 2.1.02.15.00 (CRWMS M&O 2000d, Section 6.2.5). Neutron and gamma doses considered in the screening decision for this FEP were representative of the residual radionuclide decay only and did not consider the dose from an internal criticality. Although the Zircaloy cladding is resistant to direct attack by nitric acid, cladding destabilization may occur allowing the buildup of metal-halide complexes in solutions that can promote corrosion (CRWMS M&O 2000e, p. II-1). Screening arguments for this corrosion mechanism show that environments conducive to the accumulation of the necessary chemical species are unlikely.

The NRC has also raised a question concerning effects on criticality consequence evaluations due to radiation from the criticality event (CRWMS M&O 2000i, p. 6) that was to be resolved by appropriate calculations. Nitric acid is assumed to be the principal corrosive radiolytic chemical specie. Accordingly, a scoping calculation of the possible quantity of HNO_3 produced by radiolysis during a criticality has been made with the MCNP code (CRWMS M&O 1998a) in response to this issue. The calculational method, model input description, and results from this calculation are given in the following sections.

II. Computational Method

Radiolytic production of particular chemical species depends upon the radiation environment, the chemical components present, and the physical environment where the radiolytic reactions are occurring. However, the yield of any given chemical species is characterized by a single parameter, "G", identified as the G-factor (Reed and Van Konynenburg 1991, pp. 1396-1403). The "G" value represents the number of molecules of a chemical species produced per 100 eV of absorbed radiation energy in the volume containing the irradiated environment. Measurements of the "G" factor for production of nitric acid from gamma radiation range from approximately 0.5 to 2.5 molecules/100 eV. The value used in this calculation is 1.0 and this value is also assumed to apply to neutron irradiation. The acid production rate scales linearly with the "G" factor and the uncertainty in the factor expressed in Section IV as range of possible molar quantities of nitric acid generated. The "G" value of 1.0 was chosen for this calculation to be consistent with other radiolytic acid production calculations discussed in Section IV.

For this calculation, a 21-pressurized water reactor (PWR) waste package, containing B&W 15x15 commercial spent nuclear fuel (CSNF) assemblies, was assumed to have failed and subsequently partially filled with water. The steel basket structure was assumed to have fully

degraded with the degradation products settling to the bottom of the WP. Hematite (Fe_2O_3) is assumed to be the only degradation product remaining from the basket. This is consistent with previous studies that showed that replacement of hematite by goethite had little effect on criticality. The packing fraction of the hematite was assumed to be 0.58 (CRWMS M&O 1998b, p. 15) with the remaining space filled with water. Hematite was assumed to be present outside the fuel pins in assemblies within the hematite-water mixture level but not within the guide tube spaces of those assemblies. The water level was assumed to extend to the top of the fourth row of assemblies, leaving three assemblies in the air-water vapor space at the top of the WP. The radiant energy deposition in the air-water vapor space was calculated with the MCNP code (CRWMS M&O 1998a) using the KCODE option and tracking both neutron and gamma particles. The gamma interactions include photon and electron processes.

III. Model Description

The MCNP model for the radiolysis calculation was adapted from the model developed to calculate the neutron current external to a 21-PWR waste package due to an internal criticality event (CRWMS M&O 2000f). The PWR assembly used in the referenced calculation was a Babcock and Wilcox (B&W) 15 x 15 PWR CSNF assembly. Each assembly was composed of 4 regions: the bottom end-fitting region, the active fuel region, the plenum region, and the top end-fitting region. The content of each assembly region in this model was homogenized within the region volume. Volumes and masses of material in the bottom end-fitting region, the plenum region, and the top end-fitting region were obtained from a prior shielding calculation (CRWMS M&O 2000g). Modification to this model included placing a water-Hematite mixture external to the assemblies in the lower part of the WP, adding a water moderated region above the water-Hematite mixture with an air space above the water level, and explicitly defining the fuel pins and guide tubes of assemblies in the active fuel region. As was explained above, the water-Hematite mixture was assumed to fill the region external to the fuel pins but was excluded from guide tube cells. Based on the volume of Fe in the assembly basket structure and assuming a packing fraction of 0.58 for the Hematite, the water-Hematite level has an elevation of 76.27 cm that covers the 11^{th} row of fuel pins in the 3^{rd} assembly row. The water moderator extends to an elevation of 120.32 cm at the top of the 4^{th} assembly row. This level was estimated (without iteration) to be at or slightly above the level necessary to achieve a critical configuration providing a basis for estimating the void space available for radiolytic specie production. The remaining space is filled with air at a conservative density of 1.225 kg/m^3. Use of dry air rather than an air-water vapor mixture is conservative for radiant energy deposition since the deposition depends upon the mass present and dry air maximizes the material density in the that region. The effect of including water vapor could be evaluated with additional analysis. Cross sectional views of the WP model are shown in Figures 1 and 2. Data preparation was performed with Excel spreadsheets in the file "o:\wpd\mcclure\radiolysis\21-PWR-EDAII.xls". Geometry calculations are done in the sheets "VOL-MASS" and "EDA-II.WP.rev1.dat2". Cell identifiers where the radiant energy deposition is tallied are given as follows: cell 275, external region to the three assemblies in the air space, cell 283, region external to fuel pins in the three assemblies, and cell 284, the guide tube region in the three assemblies (indicated by the white dots in Figure 2).

The energy deposition in the air filled region calculated by MCNP is given in units of MeV per gram per fission neutron. This energy must be multiplied by the mass in the deposition region, nubar (number of neutrons per fission), and number of fission events occurring in the criticality to obtain the total energy deposition from a criticality. A secondary check on the energy tallies was made by estimating the energy deposition in the specified region from the average (neutron and gamma) flux in each region multiplied by flux to dose conversion factors. These conversion factors introduce additional uncertainties and the tallies are listed for reference only.

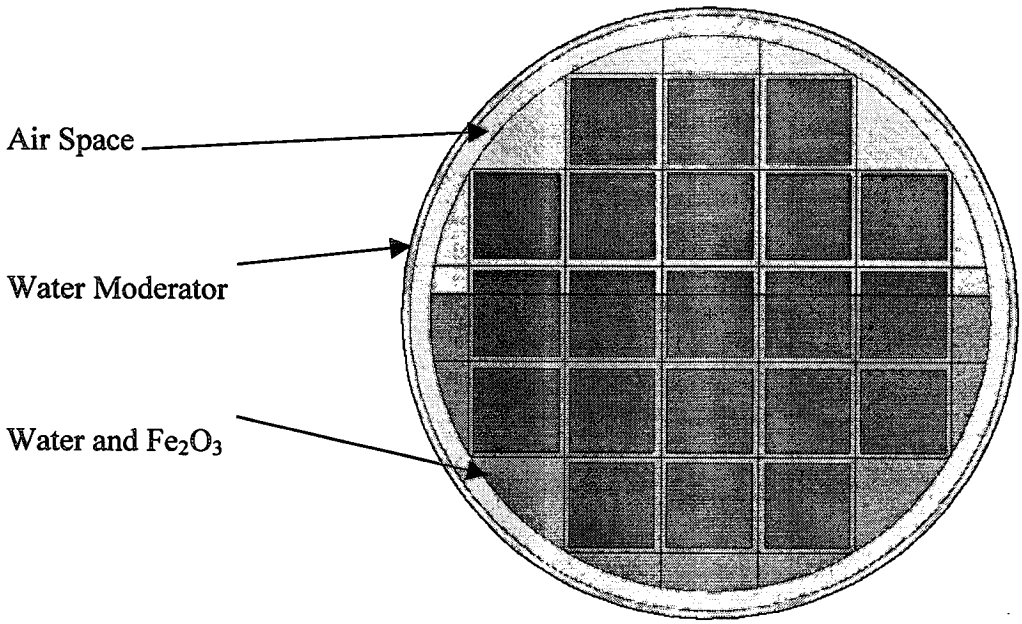

Figure 1. Cross Sectional View of 21-PWR Waste Package with Homogenized Assembly Regions

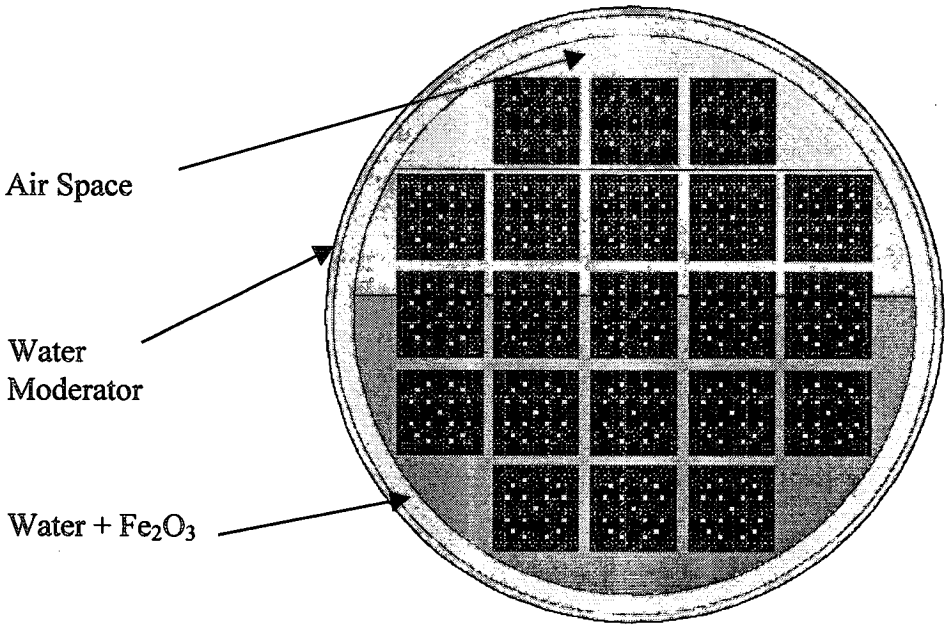

Figure 2. Cross Sectional View of the Fuel Pin Region of Assemblies in the 21-PWR Waste Package

IV. Energy Deposition Results

The radiolysis case run with the MCNP model described in Section III resulted in a k_{eff} of ~1.026. Since this case was an initial scoping one to determine if significant production of nitric acid was possible, parameters in the system were adjusted to assure that the system was critical but were not optimized further. Model revisions to better optimize the system (to a $k_{eff} \cong 1.0$ or other suitably prescribed value) for a more detailed calculation include removing the gaps between the fuel assemblies, positioning the assemblies to be in contact with the WP as appropriate for support, and specifying the end fittings explicitly rather than as homogenized regions. The radiant energy depositions in the air filled region from both the energy and flux tallies are listed in Table 1 for each cell and also the combined region (Sheet "Tally-result"). Energy tallies involve the mass in each region as compared to flux tallies that involve the volumes. Tallies are given in units of MeV per fission neutron (Total Tally Value in Table 1) for the flux tallies and in MeV per gram per fission neutron (Mean Tally Value in Table 1) for energy deposition tallies.

Table 1. Radiant Energy Deposition in Air Filled Region Within A 21-PWR WP

Cell No.	Tally type	Multiplier (Total/Mean)	Total Tally Value	Mean Tally Value	statistical error	Energy Deposition	Comparison
		Vol (cm^3) /mass (g)	MeV/fission neutron	MeV/g/fission neutron		MeV/fission neutron	Flux to Deposition
275	n-flux	560637.5637	5.4665E-04		2.6000E-03		1.0033E+01
263	n-energy	4.970014863		2.0186E-08	3.1600E-02	1.0033E-07	
162	n-energy	14.3374776		1.6375E-08	2.9800E-02	2.3477E-07	
263, 162	n-energy	19.30749247		1.7356E-08	2.4900E-02	3.3510E-07	
284	n-flux	38233.51513	5.1276E-05		3.1000E-03		1.1019E+01
275	n-energy	686.7810156		7.9334E-08	3.0000E-03	5.4485E-05	
284	n-energy	46.83605604		9.9357E-08	3.9000E-02	4.6535E-06	
283	n-energy	315.1092646		1.0235E-07	2.9000E-03	3.2253E-05	
275, 284, 283	n-energy	1048.726336		8.7145E-08	2.7000E-03	9.1391E-05	
283	n-flux	257232.0527	3.4436E-04		2.5000E-03		1.0677E+01
289	n-energy	14.76094414		1.6950E-08	2.5700E-02	2.5020E-07	
387	n-energy	42.58230848		1.2881E-08	2.3800E-02	5.4849E-07	
289, 387	n-energy	57.34325263		1.3928E-08	2.0800E-02	7.9869E-07	
294	n-energy	9.871692022		9.2691E-09	3.7700E-02	9.1502E-08	
392	n-energy	28.47781489		7.5430E-09	3.4600E-02	2.1481E-07	
294, 392	n-energy	38.34950691		7.9873E-09	2.9800E-02	3.0631E-07	
96	n-energy	137.1801781		3.9847E-09	3.5100E-02	5.4663E-07	
263	gamma-energy	4.970014863		3.8617E-08	3.5800E-02	1.9193E-07	
162	gamma-energy	14.3374776		2.5225E-08	3.8700E-02	3.6166E-07	
263, 162	gamma-energy	19.30749247		2.8672E-08	3.0100E-02	5.5359E-07	
275	gamma-energy	686.7810156		9.4934E-08	4.1000E-03	6.5199E-05	
284	gamma-energy	46.83605604		7.7581E-08	6.2000E-03	3.6336E-06	
283	gamma-energy	315.1092646		8.9838E-08	3.6000E-03	2.8309E-05	
275, 284, 283	gamma-energy	1048.726336		9.2628E-08	3.4000E-03	9.7141E-05	
275	gamma-flux	560637.5637	8.1476E-05		4.0000E-03		1.2496E+00
289	gamma-energy	14.76094414		2.0635E-08	3.5400E-02	3.0459E-07	
387	gamma-energy	42.58230848		1.8423E-08	3.1900E-02	7.8450E-07	
289, 387	gamma-energy	57.34325263		1.8993E-08	2.8100E-02	1.0891E-06	
284	gamma-flux	46.83605604	4.5233E-06		6.0000E-03		1.2448E+00
294	gamma-energy	9.871692022		1.4607E-08	4.5800E-02	1.4419E-07	

Cell No.	Tally type	Multiplier (Total/Mean)	Total Tally Value	Mean Tally Value	statistical error	Energy Deposition	Comparison
		Vol (cm^3) /mass (g)	MeV/fission neutron	MeV/g/fission neutron		MeV/fission neutron	Flux to Deposition
392	gamma-energy	28.47781489		1.3864E-08	4.2000E-02	3.9483E-07	
294, 392	gamma-energy	38.34950691		1.4056E-08	3.6800E-02	5.3902E-07	
283	gamma-flux	315.1092646	3.5267E-05		3.6000E-03		1.2458E+00
96	gamma-energy	137.1801781		8.0346E-09	3.8000E-02	1.1022E-06	
				Total		1.9380E-04	
				Neutron		9.3378E-05	
				Gamma		1.0043E-04	

The energy depositions from the flux tallies were higher than the direct energy tallies, approximately a factor of 11 for neutron and 1.25 for photons. These tallies include dose conversion factors given by

Factor = [(rem/hour)/(#/cm^2 - second)] x [(MeV/gram)/(rad/hour)] x grams/(rem/rad)

where the rem/rad term is spectrally dependent for neutrons and unity for photons. This term is a "quality" parameter for neutron radiation that relates the rem dose in phantoms to the rad value of the dose and ranges from 2 to 11. Since the void region composition differs from that of phantoms, the flux based evaluation provides only a bounding estimate of the energy deposition. The flux based energy deposition estimates were consistently higher by the factors given in the last column of Table 1 than the direct energy tallies.

The quality factors and flux-to-dose conversion are given in Table H.1 for neutrons and Table H.2 for photons (Briesmeister 1997) by energy spectra. The spectral distributions of the total conversion factors for both neutron and photons are listed in Sheet 'Tally Multipliers".

The total nitric acid production in the prescribed air space from an internal WP criticality is determined by multiplying the deposition energy per fission neutron by the number of fission neutrons in the event and the specie "G" factor. Values calculated for a transient and steady state criticality are listed in Table 2. The steady state values assumed a 1000 W power level for 1 year. These values can be linearly scaled for different powers, criticality duration times, and "G" factors.

Table 2. Radiolytic Generation of Nitric Acid from Criticality Events

Criticality Event	Energy Generated (J)	# Fissions	Radiolysis Energy (eV)	Moles HNO_3	HNO_3 (kg)
Transient Event	9.5800E+07	3.30352E+18	1.6006E+21	2.6578E-05	1.675e-06
1000 W Steady State Event (per year)	3.1558E+10	1.05896E+21	5.1308E+23	8.5198E-03	5.369e-04

The specie production rate scales as the number of fissions per unit interval and, thus, linearly for steady-state events. For a 1.0 kW steady-state criticality event extending over 10,000 years (maximum steady state duration assumed for consequence analyses), approximately 85 moles or 5.4 kg of HNO_3 could possibly be produced, assuming a "G" factor of 1.0. Uncertainty in the "G" factor results in a range of approximately 40 to 200 moles for the total acid production from the referenced steady-state criticality.

The 85-mole quantity of HNO_3 from the steady-state criticality calculation compares to approximately 13 moles or 0.82 kg of HNO_3 produced over 90,000 years at < 4 rad/hr from radionuclide decay (CRWMS M&O 2000h, Section 6.3). A second calculation of the radiolytic production of HNO_3 (CRWMS M&O 2000e, Attachment II) resulted in approximately 22.7 moles or 1.4 kg at an irradiation level of 5.0 rad/hour over 90,000 years. These latter two calculations are equivalent when adjusted for dose and air mass in the WP volume.

V. Estimated Consequences of Nitric Acid Production

The nominal value for uniform corrosion of Zircalloy-2 and -4 given in the clad degradation-localized corrosion analysis model report (AMR) (CRWMS M&O 2000j, p. 48) is approximately 8.8e-08 μm/y assuming the corrosion product is ZrO_2. The AMR provides an assessment of conditions under which zirconium and its alloys might experience enhanced corrosion rates above the nominal value. This analysis indicates that accelerated corrosion rates of zirconium are bounded by the rate derived from the fluoride concentration. The nominal corrosion rate can be enhanced in environments where the pH is less than 3.18 and the fluoride ion concentration exceeds 5 ppm (CRWMS M&O 2000j, p. 49). The fluoride concentration in J-13 water is given as 2.18 ppm (CRWMS M&O 2000c, Table 3-2.1). Fluoride concentrations in degraded waste packages containing CSNF have been estimated to range from 1.148e-04 mol/l to 9.114e-04 mol/l (CRWMS M&O 2000k, Section 6.4.3) which translate to approximately 2.2-17 ppm, thus spanning the range where accelerated zirconium corrosion could occur.

Assuming, conservatively, that the water level is maintained in the WP by equivalence between the influx drip rate and evaporation and that the nitric acid remains in the aqueous state, the concentration of HNO_3 will gradually increase by the end of the criticality to about 0.03 molar having a pH ≅ 1.5. In terms of a volume percent, the 85 moles occupy 3.57 l out of a total liquid volume of 2716 l, resulting in a 0.13 volume percent.

A mitigating factor affecting enhanced corrosion from nitric acid production during a criticality event is that its production occurs in the air space allowing dispersal outside the WP, particularly since water vapor is assumed to exit the WP to maintain the critical water level. Other factors include dilution in the water volume, dispersal by outflow from the WP, and scavenging by other materials. With respect to scavenging (likely the most important factor), nitric acid reacting with the Hematite would result in approximately 28 moles or 6.77 kg of $Fe(NO_3)_3$ based on the chemical balance

$$6\ HNO_3 + Fe_2O_3 \rightarrow 2\ Fe(NO_3)_3 + 3\ H_2O.$$

This mass constitutes less than 0.03% of the Hematite in the WP.

VI. References

Shoesmith, D.W. and King, F. 1999. *The Effects of Gamma Radiation on the Corrosion of Candidate Materials for the Fabrication of Nuclear Waste Packages.* AECL-11999. AECL Technologies, Inc. Pinawa, Manitoba, Canada.

Reed, D.T. and Van Konynenburg, R.A. 1988. *Effect of Ionizing Radiation on Moist Air Systems.* Materials Research Society Symposium Proceedings, Vol. 112. Materials Research Society, Pittsburgh, Pennsylvania.

CRWMS M&O 2000a. *Disposal Criticality Analysis Methodology Topical Report Revision 01.* YMP/TR-004Q. CRWMS M&O. Las Vegas, Nevada. ACC: MOL.20001117.0221.

CRWMS M&O 2000b. *FEPs Screening of Processes and Issues in Drip Shield and Waste Package Degradation.* ANL-EBS-PA-000002 REV 00 ICN 01. CRWMS M&O. Las Vegas, Nevada: ACC: MOL.20001211.0004.

CRWMS M&O 2000c. *Waste Form Degradation Process Model Report.* TDS-WIS-MD-000001 REV 00 ICN 01. Las Vegas, Nevada: CRWMS M&O. ACC: MOL. 20000713.0362.

CRWMS M&O 1998a. *Software Qualification Report for MCNP Version 4B2, A General Monte Carlo N-Particle Transport Code.* CSCI: 30033 V4B2LV. 30033-2003 Rev. 01. Las Vegas, Nevada: CRWMS M&O. ACC: MOL.19980622.0637.

Reed, D.T. and Van Konynenburg, R.A. 1991. *Effect of Ionizing Radiation on the Waste Package Environment.* High Level Radioactive Waste Management, Proceeding of the Second Annual International Conference. Las Vegas, Nevada. April 28-May 3, 1991. American Nuclear Society. LaGrange Park, Illinois. TIC: 204272.

CRWMS M&O 2000d. *Clad Degradation - FEPs Screening Arguments.* ANL-WIS-MD-000008 REV 00 ICN 01. Las Vegas, Nevada. CRWMS M&O. ACC: MOL.20001208.0061.

CRWMS M&O 2000e. *Summary of In-Package Chemistry for Waste Forms.* ANL-EBS-MD-000050 REV 01E. Las Vegas, Nevada. CRWMS M&O.

CRWMS M&O 2000f. *Neutron Current in a Neighboring WP due to Criticality of a Degraded 21-PWR WP.* CAL-EBS-NU-000015 REV 00A. Las Vegas, Nevada. CRWMS M&O.

CRWMS M&O 2000g. *Dose Rate Calculation for the 21-PWR UCF Waste Package.* CAL-UDC-NU-000002 REV 00. Las Vegas, Nevada: CRWMS M&O. ACC: MOL.20000223.0507.

CRWMS M&O 1998b. *Supplemental Criticality Calculations for Degraded Internal Configurations of a 21 PWR WP.* BBA000000-01717-0210-00022 REV 00. Las Vegas, Nevada: CRWMS M&O. ACC: MOL.19980919.0086.

Briesmeister, J.F., ed. 1997. *MCNP-A General Monte Carlo N-Particle Transport Code.* LA-12625-M, Version 4B. Los Alamos, New Mexico: Los Alamos National Laboratory. ACC: MOL.19980624.0328.

CRWMS M&O 2000h. *Gamma and Neutron Radiolysis in a 21-PWR Waste Package.* CAL-MGR-NU-000006 REV 00A. Las Vegas, Nevada: CRWMS M&O.

CRWMS M&O 2000i. Summary Highlights of NRC/DOE Technical Exchange and Management Meeting on Subissues Related to Criticality, October 23-25, 2000. Las Vegas, Nevada: CRWMS M&O.

CRWMS M&O 2000j. *Clad Degradation-Local Corrosion of Zirconium and its Alloys under Repository Conditions.* ANL-EBS-MD-000012 REV 00. Las Vegas, Nevada. CRWMS M&O. ACC: MOL.20000405.0479.

CRWMS M&O 2000k. *In-Package Chemistry Abstraction.* ANL-EBS-MD-000037 REV 00. Las Vegas, Nevada. CRWMS M&O. ACC: MOL.20000418.0818.